

Structural and functional anatomy of the neck musculature of the dog (*Canis familiaris*)

Amnon Sharir, Joshua Milgram and Ron Shahar

The Laboratory of Musculoskeletal Biomechanics and Applied Anatomy, Koret School of Veterinary Medicine, Hebrew University of Jerusalem, Rehovot, Israel

Abstract

The morphometric properties and the anatomical relationships of the entire musculature of the canine cervical spine are reported herein. These data were obtained from the dissection of cadavers of six dogs. Total muscle length, muscle weight, fascicle length and angles of pennation were recorded for each muscle comprising the canine cervical spine. Based upon these properties, physiological cross-section area (PCSA) and architectural index were estimated. When scaled by whole body mass, the values of each of these parameters were found to be similar between all dogs. Muscles that course from the cranial neck to the shoulder girdle or the rib cage (e.g. brachiocephalicus and rhomboideus capitis) were found to have relatively long fascicles and low PCSA values and thus appear to be designed for rapid excursions. By contrast, muscles that primarily support the neck and shoulder against gravitational forces (e.g. serratus ventralis and trapezius) were found to have relatively high PCSA values and short fascicle lengths, and thus have the capacity to generate large forces. Differences of morphometry as well as nomenclature were found between the canine and human neck musculature. Nevertheless, many similarities exist; in particular, both species have similar muscles adapted to force generation or large excursions. We thus conclude that the canine neck may be used as a modelling tool for biomechanical investigations of the human cervical region as long as the differences listed are borne in mind.

Key words anatomy; dog; morphometry; muscle; neck; PCSA.

Introduction

Numerous biomechanical investigations of the human cervical spine have been published in recent years (e.g. White et al. 1975; Deng & Goldsmith, 1987; Winters & Peles, 1990; Snijders et al. 1991; Kumaresan et al. 1999; Yoganandan et al. 2001).

The canine cervical spine has been used extensively as a model for the human cervical spine. Such studies are essential for the elucidation of biological processes that cause diseases in this body segment, the assessment of the feasibility and consequences of surgical procedures, and the evaluation of the characteristics of different fixation devices (Gooding et al. 1975; Whitehill & Barry, 1985; Panjabi et al. 1988; Sharp et al. 1989;

Villarraga et al. 1999). However, significant data relevant to the study of the canine cervical spine are lacking.

The musculature of the canine cervical spine stabilizes the head, neck and thoracic segments (Nickel et al. 1986); these muscles produce head movements, maintain posture and resist undesired perturbations. Head positioning is crucial to a wide range of activities, including visual and auditory orientation, feeding and vestibular function. In animals, activities such as grooming, predation and defence are also dependent upon head position and neck movement.

In vivo studies to determine muscle forces, loads and stresses in vertebrae are technically difficult to perform, and the data obtained from such studies are limited. Therefore, theoretical and numerical biomechanical models have been developed as tools aimed at gaining insight into the kinematics and kinetics of the cervical spine (Winters, 1988; Snijders et al. 1991; Li et al. 1995). Biomechanical models of cervical segments require knowledge of the magnitude and direction of all forces acting upon them (Keshner et al. 1997; Runciman &

Correspondence

Dr Amnon Sharir DVM, The Laboratory of Musculoskeletal Biomechanics and Applied Anatomy, Koret School of Veterinary Medicine, The Hebrew University of Jerusalem, PO Box 12, Rehovot 76100, Israel.
T: 972 8 9489756; F: 972 8 9467940; E: Sharira@agri.huji.ac.il

Accepted for publication 14 December 2005

Richmond, 1997; Cheng & Scott, 2000; Richmond et al. 2001; Gellman et al. 2002). Consequently, such models require a comprehensive database, which includes the morphometric parameters describing the architecture of each of these muscles. Analyses of such models enable the determination of clinically significant parameters, including muscle forces, intervertebral loads and intervertebral disc pressure.

The basic morphometric quantities and anatomical data required for such models consist of the total weight and length of each muscle, its fascicle length, and the orientation of its fibres (angle of pennation). Other parameters that have been reported include fibre type composition and dynamic joint angles during various activities (Zajac, 1989; Zajac & Gordon, 1989; Richmond, 1998).

A study by Kamibayashi & Richmond (1998) described the anatomy and morphometry of the muscles of the cervical spine in humans. Other studies described a similar database for non-human primates (Richmond et al. 2001), cats (Selbie et al. 1993; Richmond et al. 1999) and horses (Gellman et al. 2002). However, to the best of our knowledge, similar studies describing the anatomy and morphometry of the musculature of the canine neck are not available.

The study reported here describes the results of a comprehensive investigation of the anatomy and detailed architecture of the musculature of the canine neck. Comparison is made with the human cervical musculature. We also compare the scaled physiological cross-section area (PCSA) of equivalent human and canine muscles, and examine the association between fascicle length–PCSA and muscle function. The data presented can then be used to create biomechanical models of the canine neck and to make estimates of the muscle's capacity of force development.

Materials and methods

Specimens

The study is based on the dissection of cadavers of six young adult dogs that were put-down at a local animal shelter due to dog population control regulations (dogs A–F). The dogs were of mixed breed and well muscled, with lean to moderate body condition scores. They ranged in weight from 19 to 28 kg (mean 23.8 kg), and were estimated by their dentition to be between 2 and 5 years of age. All animals were found

Table 1 Subject data

Dog	Age (years)	Mass (kg)	Breed
A	4	25	mixed
B	3	24	mixed
C	2	19	mixed
D	4	20	mixed
E	5	27	mixed
F	2	28	mixed

to be healthy by ante-mortem physical examination. The details of all dogs used in this study are listed in Table 1.

Dissection

Immediately following euthanasia, the skin and subcutaneous tissues of the right forequarter were carefully removed. Each of the muscles of the right-hand side of the neck was identified, carefully isolated and removed. Measurements and evaluations were performed within hours of euthanasia, and thus were not significantly affected by rigor mortis. Duration of each dissection ranged between 5 and 7 h. Tissues were kept moist with physiological saline (0.9%) throughout the dissection and measurement processes. The list of muscles studied is given in Table 2.

Muscle parameters

Immediately after removal of superficial fat and fascia, each muscle was weighed with an electronic digital scale, thus avoiding dehydration artefacts. Measurement precision was ± 0.01 g. Total muscle length was defined as the overall distance between (but not including) the muscle's tendinous attachments. Each muscle was placed on a flat dissection surface, and its length measured with a flexible tape measure, so that curved surfaces could be followed (Kamibayashi & Richmond, 1998). Measurement precision was ± 0.05 cm. Pennation angle, defined as the angle formed between the direction of muscle fascicles and the line connecting the muscle's origin and insertion, was evaluated with a protractor. Measurement precision was $\pm 2^\circ$. Muscles with varying pennation angles were sampled at five sites from different regions within the muscle, and the average angle was determined by calculating the arithmetic mean (Lieber & Friden, 2000).

Table 2 Total mass, length and pennation angle of canine neck muscles

Muscle	Abbreviation	n	Muscle mass (g)			Total muscle length (cm)			Pennation angle (°)
			Mean	(SD)	Range	Mean	(SD)	Range	
Trapezius – cervical portion	TR	6	31.11	(8.29)	22.03–45.06	12.68	(2.39)	9.1–15.1	0–12 (6)
Brachiocephalicus	Br	6	91.47	(17.15)	73.13–117.04	28.67	(3.22)	24.7–33.5	0–5
Omotransversarius	OM	6	36.94	(6.90)	29.29–45.6	16.87	(2.76)	14.8–20.8	0–5
Rhomboideus capitis	RCP	6	6.23	(1.34)	4.46–8.23	18.00	(2.90)	15.1–22.1	0–5
Rhomboideus cervicis	RC	6	28.10	(7.90)	17–37.12	17.47	(4.21)	12.8–22.1	0–40 (20)
Serratus ventralis cervicis C ₂	SV.C ₂	4	9.13	(6.06)	5.04–17.9	14.05	(3.87)	9.6–17.9	0–5
Serratus ventralis cervicis C ₃	SV.C ₃	6	13.32	(6.89)	6.29–26.25	11.20	(3.20)	7.5–15.7	0–5
Serratus ventralis cervicis C ₄	SV.C ₄	6	10.68	(3.72)	6.51–17.6	9.98	(2.63)	7.1–14.1	0–5
Serratus ventralis cervicis C ₅	SV.C ₅	6	17.15	(5.46)	12.35–26.98	9.20	(2.18)	6.8–12.5	0–5
Serratus ventralis cervicis C ₆	SV.C ₆	6	13.65	(3.75)	8.45–17.15	8.12	(1.57)	6.6–10.7	0–20 (10)
Serratus ventralis cervicis C ₇	SV.C ₇	6	15.17	(3.23)	10.83–19.19	8.20	(1.28)	6.5–9.8	0–25 (12.5)
Splenius	SP	6	95.36	(25.26)	53.57–121.65	22.67	(5.63)	17.8–32.6	0–35 (17.5)
Longissimus capitis	LC	6	23.52	(7.52)	11.32–32.65	19.57	(5.70)	14.2–29.5	0–10
Longissimus cervicis C ₃	LCV.C ₃	5	8.31	(3.96)	3.4–13.35	11.08	(1.93)	9.1–13.7	0–5
Longissimus cervicis C ₄	LCV.C ₄	5	10.68	(4.05)	6.12–17.07	11.30	(2.26)	8.8–14.5	0–35 (17.5)
Longissimus cervicis C ₅	LCV.C ₅	5	10.77	(5.29)	5.82–18.29	12.17	(2.84)	8–15.6	0–25 (12.5)
Longissimus cervicis C ₆	LCV.C ₆	5	9.61	(5.01)	4.93–15.96	11.63	(2.74)	8.5–16.1	0–5
Spinalis et semispinalis	SST & SSC	6	30.99	(8.24)	22.89–45.91	20.52	(4.23)	17–28.4	0–5
Biventer cervicis	BC	6	65.31	(15.76)	50.21–84.65	24.35	(4.42)	20.7–31.3	0–5
Complexus C ₃ –C ₄	COMP.C ₃₋₄	6	17.67	(5.68)	12.77–28.06	13.30	(2.68)	9.5–16.4	0–5
Complexus C ₅	COMP.C ₅	5	8.06	(3.73)	3.97–12.74	13.15	(2.84)	9.4–15.4	0–5
Complexus C ₆	COMP.C ₆	5	8.02	(2.16)	5.61–10.29	13.73	(3.14)	9.3–16.5	0–5
Complexus C ₇	COMP.C ₇	6	9.74	(2.95)	5.77–13.75	15.76	(3.52)	9.6–18.4	0–5
Complexus T ₁	COMP.T ₁	5	10.88	(4.54)	7.1–18.19	13.25	(2.43)	11.2–16.5	0–5
Intertransversarii cervicis	IC	5	48.48	(10.74)	38.19–66.54	16.46	(2.34)	13.9–20.1	0–35 (17.5)
Multifidus cervicis	MC	5	26.14	(6.91)	17.23–32.15	13.14	(2.73)	10.0–17.0	0–40 (20)
Sterno-occipitalis	SO	5	23.34	(9.22)	13.72–35.06	16.48	(2.46)	14.1–20.4	0–5
Sternomastoideus	SM	5	32.12	(10.83)	16.49–43.13	16.34	(2.12)	13.9–19.3	0–5
Sternohyoideus	SH	5	20.09	(–4.85)	15.13–26.28	16.08	(–2.30)	14.2–19.8	0–5
Sternothyroideus	ST	5	10.75	(–5.81)	5.83–19.49	15.48	(–2.50)	11.5–17.5	0–5
Scalenus supercostalis dorsalis	SSD	5	11.27	(2.73)	6.36–15.15	11.62	(2.56)	9.5–16.9	0–5
Scalenus supercostalis intermedius	SSI	5	13.21	(5.29)	8.37–21.07	14.20	(3.35)	12.0–20.1	0–5
Scalenus supercostalis ventralis	SSV	5	5.59	(2.06)	2.21–12.01	8.26	(2.50)	5.8–12.4	0–5
Scalenus primae costae dorsalis	SPD	5	1.00	(0.40)	0.61–1.52	2.08	(0.44)	1.1–2.7	0–45 (22.5)
Scalenus primae costae intermedius	SPI	5	2.50	(1.76)	1.35–5.69	3.98	(1.18)	2.9–5.8	0–5
Scalenus primae costae ventralis	SPV	5	3.67	(1.69)	1.9–6.15	5.66	(0.48)	5–6.1	0–5
Longus capitis C ₂	LCP.C ₂	5	10.95	(3.48)	6.15–13.75	7.80	(1.11)	6.7–9.3	0–5
Longus capitis C ₂₋₃	LCP.C ₂₋₃	5	12.27	(4.63)	6.8–18.84	9.62	(2.26)	7–12.9	0–5
Longus capitis C ₄₋₅₋₆	LCP.C ₄₋₅₋₆	5	23.09	(7.05)	15.72–31.8	13.28	(3.16)	8.3–16.5	0–5
Longus colli C ₁ –C ₄	LCO.C ₁₋₄	5	7.02	(2.13)	3.87–9.43	5.86	(0.63)	5.4–6.6	0–20 (10)
Longus colli C ₂ –C ₅	LCO.C ₂₋₅	5	8.37	(2.43)	6.77–12.6	6.04	(0.78)	5.2–7.1	0–20 (10)
Longus colli C ₃ –C ₆	LCO.C ₃₋₆	4	12.50	(3.35)	8.26–17.21	7.46	(1.21)	5.6–8.8	0–20 (10)
Longus colli C ₆ –C ₇	LCO.C ₆₋₇	4	4.10	(0.93)	2.85–4.94	4.90	(0.49)	4.3–5.6	0–20 (10)
Longus colli C ₇ –T ₁	LCO.C _{7-T1}	4	4.10	(1.35)	2.83–6.35	4.12	(1.24)	2.0–5.2	0–20 (10)
Rectus capitis latetralis	RCL	4	1.36	(0.27)	1.11–1.73	3.08	(0.59)	2.6–3.8	0–5
Rectus capitis ventralis	RCV	3	0.94	(0.12)	0.81–1.04	3.00	(0.26)	2.7–3.2	0–5
Rectus capitis dorsalis Major	RCD.Major	5	8.54	(3.17)	5.23–12.57	7.78	(1.20)	6.2–9.3	0–5
Rectus capitis dorsalis Intermedius	RCD.Inter	5	4.95	(1.25)	3.44–6.42	4.80	(1.01)	3.8–6.5	0–20 (10)
Rectus capitis dorsalis Minor	RCD.Minor	5	1.97	(0.79)	1.18–3.29	2.62	(0.74)	1.6–3.4	0–5
Oblique capitis caudalis	OCC	5	38.22	(10.90)	26.81–49.59	5.86	(0.73)	5–6.8	0–5
Oblique capitis carnialis principle	OCCrP	5	7.80	(2.65)	4.46–10.6	5.34	(0.84)	4.3–6.3	0–5
Oblique capitis carnialis accessory	OCCrA	5	4.58	(0.55)	4.02–5.21	4.60	(0.74)	3.9–5.5	0–5

Note: n represents number of dogs evaluated. Pennation angle is represented as the range of five individual measurements, and the mean is provided in parentheses where the range exceeds 0–10°.

Muscle fascicles are defined as bundles of 20–50 muscle fibres (Sacks & Roy, 1982). Their length was determined using the protocol described by Sacks & Roy (1982). Briefly, each muscle was placed in 10% formalin for 48–72 h. It was then soaked in 0.4 M phosphate-buffered saline solution, at a pH of 7.2, for 24–48 h, and then placed in 10% sulfuric acid solution for 3–7 days until fascicles could be teased apart easily. Fixation of muscles with an embalming solution similar to the solution used in this study was shown to cause negligible (< 5%) shrinkage of muscle fibres (Cuts, 1988). Using surgical forceps and scalpel, a fascicle was dissected from the muscle and its length was measured with a flexible tape measure. Measurement precision was ± 0.05 cm. Muscles in which fascicle length appeared to be non-uniform were represented by averaging lengths from 3–8 fascicles dissected at various locations. The most superficial fascicles were avoided because they tend to be slightly longer than fascicles within the muscle belly (Kamibayashi & Richmond, 1998).

Normalization of fascicle lengths was carried out in one dog (chosen at random – dog F) by measuring individual sarcomere lengths in fascicles obtained from each cervical muscle. This process was performed bilaterally so that sarcomere lengths could be compared between each muscle on the right side and its corresponding muscle on the left side. Biopsies were obtained from 1–5 representative sites throughout each muscle, with the aid of a stereomicroscope. Excised fibres were mounted on a glass slide, coverslipped using glycerol and evaluated by a light microscope (Nikon E800) with a 100 \times oil-immersion objective. A high-resolution image (Nikon DXM 1200) was processed by image processing software (Image-pro plus 5.0). Sarcomere length was calculated as the mean of measurements made at 20–60 random locations throughout the fibre (see for example Fig. 1). The mean measured fascicle length was then corrected by multiplying it by the ratio of the measured sarcomere length and the optimal canine sarcomere length, assumed to be 2.5 μm (Herzog et al. 1992; W. Herzog, personal communication, 2004).

PCSA is the ratio between muscle volume and effective fascicle length (Wickiewicz et al. 1983; Raikova & Prilutsky, 2001). It reflects the number of sarcomeres lying in parallel, and is therefore proportional to the amount of force the muscle can generate. The PCSA of each muscle was calculated according to the following equation:

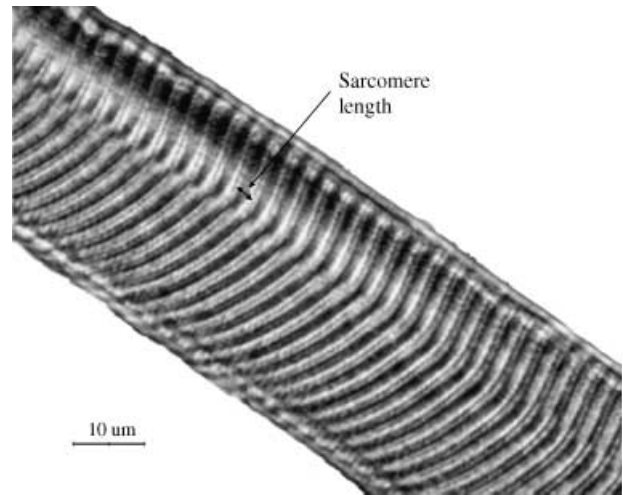


Fig. 1 Image to show method for measuring sarcomere length (right trapezius, dog E) using light microscope. The mean sarcomere length for this muscle was found to be 3.08 μm ($\times 100$).

$$\text{PCSA} = (m \cos \theta) / \rho l \quad (1)$$

where m is the muscle mass (g), θ is the average angle of pennation for the muscle fascicle (degrees), l is the muscle fascicle length (cm), and ρ is the muscle tissue density (g cm^{-3}). A uniform density of 1.06 g cm^{-3} was assumed (Mendez & Keys, 1960).

Architectural index (AI) reflects the number of sarcomeres in series in a muscle, and is proportional to the potential velocity of muscle contraction. The AI of each muscle is defined as the ratio between the muscle's fascicle length and the total length of the muscle:

$$\text{AI} = l / L \quad (2)$$

where l is the muscle fascicle length (cm) and L is total muscle length (cm).

Muscles with small areas of attachment were considered single units, exerting force in a straight line connecting their origin and insertion. Muscles with multiple or large attachment sites were divided based on anatomical features, with each division considered as a separate unit.

In order to facilitate comparisons between muscles in different species with those of humans, Richmond et al. (2001) recommended a scaling procedure for the values of PCSA. This scaling procedure assumes that the geometry of the musculature of both species is similar in principal, and therefore the conversion of parameters

of linear dimensions from dog to humans is based on the third root of their weight ratios. For area dimensions, such as PCSA, the linear scaling ratio is squared (Schmidt-Nielsen, 1984; Richmond et al. 2001). In this study, linear scaling was based on the average weight of the dogs (23.8 kg) relative to the average weight of human specimens used by Richmond et al. (64 kg) and is therefore 1 : 1.39 (linear dimension); for area dimensions, such as PCSA, this scaling factor is squared, and is 1 : 1.93 (linear dimension²).

To determine whether the morphometric parameters could be extrapolated to dogs of different sizes, muscle mass, PCSA and fascicle length were scaled by whole body mass assuming geometric similarity. Muscle mass was scaled as a fraction of body mass (g kg^{-1}), PCSA as a fraction of body mass^{2/3} ($\text{cm}^2 \text{kg}^{-2/3}$), and fascicle length as a fraction of body mass^{1/3} ($\text{cm kg}^{1/3}$).

Results

The presentation of the results of this study follows the form suggested by Kamibayashi & Richmond (1998) in order to facilitate comparison with results reported for humans and non-human primates. Anatomical data and morphometric parameters for all muscles dissected from the right side of each of the six dogs used in this study are listed in Tables 2 and 3. Comparison between muscles of the right and left sides is presented in

Table 4. The parameters presented include total muscle mass, total muscle length, pennation angle, fascicle length, PCSA and AI. In order to ensure precision, the lengths of the muscles were measured both *in situ* and after dissection, and results were compared. Differences were found to be less than 5%. For those muscles consisting of several subunits, the data are presented for each subunit.

Muscle mass, PCSA and fascicle length data were scaled assuming geometric similarity (Table 5). For each of the three parameters, the scaled values of all subjects were quite similar (see Table 5a–c).

A comparison of the scaled values of PCSA between humans and dogs is presented in Fig. 2. The ordinate represents the values of PCSA of muscles in humans, and the abscissa represents the values of PCSA of the same muscles in the dog. Therefore, muscles whose value falls on the diagonal are those where the PCSA is the same in both species, those below the diagonal line have higher PCSA values in the dog, and those above the diagonal line have larger PCSA values in humans.

The relationship between PCSA (which is proportional to maximal muscle force capacity) and fascicle length (proportional to maximum muscle excursion) is presented in Fig. 3. Those muscles characterized by long fascicles and small PCSA, and those muscles characterized by short fascicles and large PCSA are surrounded by circles (Lieber & Friden, 2000, 2001).

Fig. 2 Comparison of scaled PCSA values between dogs and humans (human data obtained from Kamibayashi & Richmond, 1998). Muscle abbreviations: TR, trapezius – cervical portion; BR, brachiocephalicus; SO, sterno-occipitalis; SM, sternomastoideus; RC, rhomboideus capitis and rhomboideus cervicis; SV, serratus ventralis cervicis; SP, splenius, BC, biventer cervicis; SS, scalenus supracostalis; SP, scalenus primae costae; LCP, longus capitis; OCC, oblique capitis caudalis; RCL, rectus capitis lateralis; RCD.Maj., rectus capitis dorsalis major; RCD.Int., rectus capitis dorsalis intermedius. Due to differences in nomenclature and anatomy between these species, the chart relates only to those muscles which were found to share similar function and structure. PCSA values of several muscles are summed (e.g. the human BR muscle is equivalent to the sum of the canine BR, SO and SM muscles), in order to enable comparison between muscles of the dog and human.

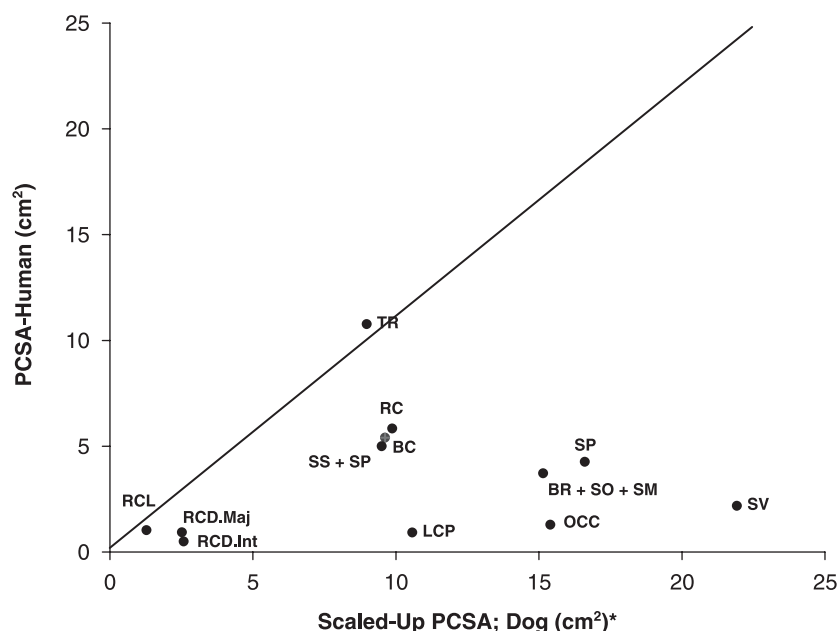


Table 3 Fascicle lengths, PCSA and AI of canine neck muscles

Muscle	Abbreviation	n	Fascicle length (cm)			PCSA (cm ²)			AI (cm cm ⁻¹)		
			Mean	(SD)	Range	Mean	(SD)	Range	Mean	(SD)	Range
Trapezius – cervical portion	TR	6	6.5	(4.52)	1.7–13.2	4.63	(1.29)	3.50–6.82	0.52	(0.07)	0.40–0.59
Brachiocephalicus	Br	6	21.0	(4.78)	16.0–31.4	4.27	(1.24)	3.28–5.97	0.74	(0.10)	0.60–0.86
Omotransversarius	OM	6	13.7	(3.55)	11.1–20.5	2.66	(0.62)	2.12–3.70	0.83	(0.09)	0.76–0.98
Rhomboideus capitis	RCP	6	14.0	(2.88)	11.6–19.4	0.42	(0.12)	0.32–0.63	0.81	(0.08)	0.70–0.92
Rhomboideus cervicis	RC	6	5.9	(2.98)	2.9–12.9	4.67	(2.05)	2.31–7.39	0.37	(0.17)	0.21–0.57
Serratus ventralis cervicis C ₂	SV.C ₂	4	10.2	(4.03)	6.6–15.6	0.64	(0.13)	0.55–0.72	0.78	(0.12)	0.70–0.92
Serratus ventralis cervicis C ₃	SV.C ₃	6	8.8	(2.41)	5.8–13.4	1.54	(0.78)	0.97–2.88	0.94	(0.22)	0.77–1.33
Serratus ventralis cervicis C ₄	SV.C ₄	6	7.7	(1.71)	6.0–11.3	1.34	(0.51)	0.82–2.06	0.84	(0.06)	0.76–0.91
Serratus ventralis cervicis C ₅	SV.C ₅	6	7.0	(1.39)	5.3–10.0	2.30	(0.83)	1.58–3.72	0.83	(0.03)	0.79–0.87
Serratus ventralis cervicis C ₆	SV.C ₆	6	5.5	(0.78)	3.9–6.3	2.19	(0.54)	1.40–2.74	0.73	(0.13)	0.59–0.87
Serratus ventralis cervicis C ₇	SV.C ₇	6	4.2	(0.69)	3.2–5.5	3.29	(0.37)	2.70–3.71	0.53	(0.08)	0.45–0.65
Splenius	SP	6	9.5	(6.98)	2.5–20.4	8.56	(2.22)	5.96–12.00	0.50	(0.11)	0.43–0.70
Longissimus capitis	LC	6	3.9	(1.13)	1.4–13.4	5.45	(1.72)	3.29–7.42	0.22	(0.04)	0.17–0.29
Longissimus cervicis C ₃	LCV.C ₃	5	9.6	(2.02)	6.8–13.2	0.60	(0.16)	0.44–0.82	0.75	(0.22)	0.41–0.93
Longissimus cervicis C ₄	LCV.C ₄	5	7.4	(2.75)	3.0–12.0	1.25	(0.73)	0.73–2.37	0.73	(0.19)	0.43–0.82
Longissimus cervicis C ₅	LCV.C ₅	5	6.3	(1.27)	4.5–8.8	1.64	(1.00)	0.72–3.11	0.63	(0.18)	0.35–0.82
Longissimus cervicis C ₆	LCV.C ₆	5	6.1	(3.38)	3.1–13.7	1.51	(0.99)	0.52–2.86	0.55	(0.25)	0.35–0.97
Spinalis et semispinalis	SST & SSC	6	14.4	(3.10)	10.9–19.5	2.09	(0.38)	1.48–2.48	0.69	(0.14)	0.55–0.84
Biventer cervicis	BC	6	12.9	(3.91)	8.1–20.7	4.96	(4.31)	3.76–6.52	0.52	(0.08)	0.44–0.59
Complexus C ₃ –C ₄	COMP.C ₃₋₄	6	7.9	(2.81)	5.5–12.9	2.12	(0.17)	1.90–2.28	0.57	(0.15)	0.40–0.73
Complexus C ₅	COMP.C ₅	5	10.0	(2.52)	7.5–13.5	0.58	(0.18)	0.46–0.79	0.78	(0.13)	0.63–0.86
Complexus C ₆	COMP.C ₆	5	10.9	(3.28)	7.8–15.2	0.62	(0.03)	0.59–0.65	0.82	(0.13)	0.68–0.91
Complexus C ₇	COMP.C ₇	6	9.9	(4.31)	2.5–15.9	0.90	(0.27)	0.64–1.28	0.70	(0.22)	0.49–0.90
Complexus T ₁	COMP.T ₁	5	9.6	(0.87)	8.1–10.5	0.79	(0.06)	0.74–0.85	0.80	(0.15)	0.62–0.89
Intertransversarii cervici	IC*										
Multifidus cervicis	MC*										
Sterno-occipitalis	SO	5	15.0	(2.15)	12.8–18.6	1.43	(0.43)	0.92–1.82	0.92	(0.03)	0.89–0.97
Sternomastoideus	SM	5	14.8	(2.82)	9.8–18.3	2.11	(0.69)	1.42–3.23	0.88	(0.09)	0.73–0.95
Sternohyoideus	SH	5	14.9	(2.70)	13.6–18.8	1.32	(0.43)	0.92–1.97	0.92	(0.09)	0.77–0.97
Sternothyroideus	ST	5	14.9	(2.61)	13.4–17.4	0.74	(0.54)	0.36–1.66	0.96	(0.07)	0.89–1.07
Scalenus supercostalis dorsalis	SSD	5	9.5	(2.36)	7.6–14.9	1.07	(0.25)	0.75–1.40	0.81	(0.07)	0.71–0.88
Scalenus supercostalis intermedius	SSI	5	11.5	(3.90)	7.0–19.5	1.06	(0.18)	0.79–1.29	0.79	(0.09)	0.66–0.88
Scalenus supercostalis ventralis	SSV	5	6.2	(1.74)	5.0–10.5	0.65	(0.23)	0.41–1.01	0.76	(0.06)	0.71–0.86
Scalenus primae costae dorsalis	SPD	5	1.6	(0.53)	0.9–2.5	0.60	(0.20)	0.32–0.91	0.77	(0.11)	0.66–0.89
Scalenus primae costae intermedius	SPI	5	2.7	(0.75)	2.0–4.2	0.77	(0.20)	0.58–1.10	0.79	(0.11)	0.61–0.88
Scalenus primae costae ventralis	SPV	5	4.9	(0.66)	4.2–6.3	0.75	(0.27)	0.40–1.02	0.85	(0.07)	0.75–0.95
Longus capitis C ₂	LCP.C ₂	5	5.1	(2.00)	2.5–8.4	2.34	(1.24)	0.78–3.74	0.64	(0.15)	0.46–0.80
Longus capitis C ₂₋₃	LCP.C ₂₋₃	5	5.6	(1.18)	3.3–7.5	2.23	(1.31)	1.18–4.34	0.60	(0.16)	0.39–0.78
Longus capitis C ₄₋₅₋₆	LCP.C ₄₋₅₋₆	5	8.5	(2.89)	3.2–12.5	2.64	(0.96)	1.64–4.04	0.66	(0.16)	0.43–0.80
Longus colli C ₁ –C ₄	LCO.C ₁₋₄	5	2.1	(0.33)	1.6–2.7	3.07	(0.70)	2.05–3.65	0.36	(0.03)	0.32–0.41
Longus colli C ₂ –C ₅	LCO.C ₂₋₅	5	2.0	(0.50)	0.9–2.6	3.82	(0.57)	3.31–4.78	0.34	(0.06)	0.27–0.41
Longus colli C ₃ –C ₆	LCO.C ₃₋₆	4	2.2	(0.55)	1.3–2.8	4.85	(1.53)	2.90–6.15	0.33	(0.09)	0.27–0.47
Longus colli C ₆ –C ₇	LCO.C ₆₋₇	4	1.8	(0.44)	1.3–2.5	2.40	(0.33)	2.15–2.89	0.35	(0.05)	0.30–0.39
Longus colli C ₇ –T ₁	LCO.C _{7-T1}	4	1.7	(0.18)	1.5–1.9	2.34	(1.06)	1.66–3.93	0.49	(0.29)	0.29–0.93
Rectus capitis latetralis	RCL*										
Rectus capitis ventralis	RCV*										
Rectus capitis dorsalis Major	RCD.Major	5	6.3	(1.19)	4.9–8.3	1.30	(0.55)	0.95–2.26	0.81	(0.06)	0.71–0.87
Rectus capitis dorsalis Intermedius	RCD.Inter	5	3.6	(1.06)	2.2–5.4	1.30	(0.34)	0.99–1.79	0.60	(0.08)	0.41–0.74
Rectus capitis dorsalis Minor	RCD.Minor	5	1.6	(0.46)	1.0–2.4	1.21	(0.28)	0.77–1.43	0.60	(0.13)	0.41–0.74
Oblique capitis caudalis	OCC	5	4.6	(1.25)	3.0–6.6	7.94	(2.54)	5.92–12.08	0.79	(0.06)	0.70–0.85
Oblique capitis carnialis principle	OCCrP	5	2.3	(0.57)	1.3–3.2	3.37	(1.43)	1.79–5.13	0.44	(0.11)	0.32–0.55
Oblique capitis carnialis accessory	OCCrA	5	2.3	(0.30)	1.9–2.8	1.88	(0.19)	1.60–2.05	0.51	(0.05)	0.45–0.57

PCSA, physiological cross-section area; AI, architectural index; n, number of dogs evaluated.

*Four muscles do not have values reported in this table.

Table 4 Parameters obtained from the bilateral dissection of dog F

Muscle name	Muscle length (cm)		Muscle mass (g)		Mean fascicle length (cm)		Sarcomere length (µm)				Normalized fascicle length (cm)		Normalized PCSA (cm ²)	
	Left	Right	Left	Right	Left	Right	Left Mean	Range	Right Mean	Range	Left	Right	Left	Right
Trapezius – cervical portion	15.8	15.1	32.78	29.59	7.40	8.38	2.26	(1.63–2.88)	3.08	(2.61–3.35)	8.19	6.80	3.78	4.11
Brachiocephalicus – entire muscle	30.2	30.9	86.90	88.34	27.42	25.97								
Cleidobrachialis			28.18	28.62	10.60	10.30	2.26	(1.94–2.59)	2.56	(2.13–2.91)	11.73	10.06	2.27	2.69
Cleidomastoideus			25.24	27.17	16.95	17.35	1.91	(1.76–2.12)	2.21	(1.98–2.63)	22.19	19.63	1.07	1.31
Cleidocervicalis			33.48	32.55	15.80	16.00	2.75	(2.32–3.16)	2.85	(2.27–3.54)	14.36	14.04	2.20	2.19
Omotransversarius	23.2	20.0	33.15	33.64	19.95	18.55	2.91	(2.64–3.32)	2.28	(1.83–2.84)	17.14	20.34	1.83	1.56
Rhomboideus capitis	20.5	22.1	5.58	6.75	18.05	19.95	2.26	(2.02–2.46)	2.55	(2.36–2.86)	19.97	19.56	0.26	0.33
Rhomboideus cervicis	22	22.1	42.28	37.12	6.39	6.37	1.97	(1.60–2.48)	2.85	(2.42–3.28)	8.11	5.59	4.92	6.27
Serratus ventralis cervicis C ₃	16.8	15.7	11.72	9.35	14.55	13.80	2.16	(1.85–2.48)	2.04	(1.72–2.38)	16.84	16.91	0.66	0.52
Serratus ventralis cervicis C ₄	14.3	14.1	11.36	10.45	12.25	12.10	2.35	(2.13–2.53)	2.48	(2.19–2.92)	13.03	12.20	0.82	0.81
Serratus ventralis cervicis C ₅	12.6	12.5	16.85	17.80	10.67	12.23	2.29	(2.13–2.45)	2.97	(1.98–3.49)	11.65	10.29	1.37	1.63
Serratus ventralis cervicis C ₆	11.2	10.7	15.00	16.75	8.68	8.53	2.32	(1.88–2.72)	2.67	(2.15–3.23)	9.35	7.99	1.51	1.98
Serratus ventralis cervicis C ₇	10.6	9.8	19.32	16.71	6.66	5.52	1.72	(1.52–2.14)	1.88	(1.60–2.14)	9.68	7.34	1.88	2.15
Scalenus supercostalis dorsalis	19.5	16.9	10.16	15.15	16.20	14.90	2.72	(2.34–2.93)	3.18	(2.79–3.50)	14.89	11.71	0.64	1.22
Scalenus supercostalis intermedius	20.3	19.5	18.30	14.76	17.95	18.05	1.96	(1.65–2.14)	2.74	(2.40–3.14)	22.90	16.47	0.75	0.85
Scalenus supercostalis ventralis	13.4	12.4	10.82	12.01	8.21	7.07	2.73	(2.50–3.22)	2.88	(2.26–3.33)	7.52	6.14	1.36	1.85
Scalenus prima costae dorsalis	1.7	1.1	0.83	0.61	1.40	1.30	2.61	(2.40–2.77)	2.77	(2.22–3.20)	1.34	1.17	0.58	0.49
Scalenus prima costae intermedius	3.8	3.0	1.65	1.35	3.40	2.90	2.24	(1.97–2.43)	2.65	(2.33–3.01)	3.79	2.74	0.41	0.47
Scalenus prima costae ventralis	6.6	6.1	3.96	2.50	5.70	4.46	1.51	(1.38–1.77)	2.39	(1.93–2.72)	9.44	4.67	0.40	0.51
Longissimus capitis	31.1	29.5	33.22	32.65	8.78	9.06	2.12	(1.45–2.46)	2.46	(2.14–2.67)	10.35	9.21	3.03	3.35
Splenius	33.4	32.6	106.98	110.72	13.88	13.20	2.10	(1.58–2.60)	2.72	(2.23–3.21)	16.52	12.13	6.11	8.62
Biventer cervicis	30.5	31.3	75.77	74.33	18.50	17.43	2.32	(1.41–3.25)	2.80	(2.15–3.36)	19.94	15.56	3.59	4.51
Longissimus cervicis C ₃	11.8	10.2	10.30	13.35	6.53	8.15	2.15	(1.74–2.42)	3.14	(2.82–3.53)	7.59	6.49	1.28	1.94
Longissimus cervicis C ₄	13.8	13.3	10.42	11.28	12.87	12.70	2.12	(1.76–2.57)	3.07	(2.55–3.54)	15.18	10.34	0.65	1.03
Longissimus cervicis C ₅	13.7	14.2	5.60	5.82	10.10	9.95	2.19	(1.93–2.41)	3.02	(1.84–3.69)	11.53	8.24	0.46	0.67
Longissimus cervicis C ₆	13.4	16.1	18.05	15.96	5.65	5.95	1.97	(1.68–2.49)	3.03	(2.29–3.45)	7.17	4.91	2.38	3.07
Spinalis et semispinalis – cervicis	19.4	18.5	19.22	17.71	3.64	2.58	3.03	(2.58–3.35)	2.84	(2.48–3.29)	3.00	2.27	6.04	7.36
Spinalis et semispinalis – thoracis	14.2	13.4	21.03	15.42	14.00	15.20	2.24	(1.91–2.75)	3.02	(2.67–3.52)	15.63	12.58	1.27	1.16
Complexus – entire muscle	28.5	27.4	59.34	61.82									7.31	8.52
Complexus C ₄₋₃			15.95	15.44	14.80	11.80	2.00	(1.59–2.92)	2.17	(1.68–2.74)	18.50	13.59	0.81	1.07
Complexus C ₅			8.2	7.81	16.15	13.25	2.00		2.17		20.19	15.26	0.38	0.48
Complexus C ₆			10.53	10.29	17.45	14.00	2.00		2.17		21.81	16.13	0.46	0.60
Complexus C ₇			11.3	10	17.60	15.65	2.00		2.17		22.00	18.03	0.49	0.52
Complexus T ₁			14.49	18.2	19.90	17.85	2.00		2.17		24.88	20.56	0.55	0.84

Note: Data regarding brachiocephalicus and complexus are provided both for the entire muscle and for its anatomical subunits.

Table 5 Muscle mass, PCSA and fascicle length as a fraction of body mass

(a) Muscle mass (g) as a fraction of body mass (kg)

Muscle	Subject						Mean	SD
	A	B	C	D	E	F		
Trapezius – cervical portion	1.80	1.28	1.16	1.21	1.30	1.06	1.30	0.26
Brachiocephalicus	4.68	3.91	3.85	3.67	3.82	3.16	3.85	0.49
Omotransversarius	1.77	1.59	1.54	1.54	1.69	1.20	1.55	0.20
Rhomboideus capitis	0.33	0.26	0.27	0.22	0.25	0.24	0.26	0.04
Rhomboideus cervicis	1.45	1.26	1.19	0.85	0.94	1.33	1.17	0.23
Serratus ventralis cervicis C ₂	NM	0.21	NM	0.25	0.31	0.64	0.35	0.19
Serratus ventralis cervicis C ₃	1.05	0.47	0.33	0.63	0.52	0.33	0.56	0.27
Serratus ventralis cervicis C ₄	0.70	0.43	0.46	0.33	0.39	0.37	0.45	0.13
Serratus ventralis cervicis C ₅	1.08	0.58	0.65	0.66	0.69	0.64	0.72	0.18
Serratus ventralis cervicis C ₆	0.69	0.50	0.57	0.42	0.62	0.60	0.57	0.09
Serratus ventralis cervicis C ₇	0.77	0.45	0.63	0.76	0.64	0.60	0.64	0.12
Splenius	4.87	4.11	2.82	3.90	4.06	3.95	3.95	0.66
Longissimus capitis	1.01	0.95	0.60	0.99	1.09	1.17	0.97	0.20
Longissimus cervicis C ₃	0.44	0.21	0.18	0.32	0.40	0.48	0.34	0.12
Longissimus cervicis C ₄	0.68	0.41	0.32	0.34	0.48	0.40	0.44	0.13
Longissimus cervicis C ₅	0.65	0.43	0.43	0.30	0.68	0.21	0.45	0.19
Longissimus cervicis C ₆	0.27	0.34	0.31	0.25	0.59	0.57	0.39	0.15
Spinalis et semispinalis	1.10	1.05	1.20	1.57	1.70	1.18	1.30	0.27
Biventer cervicis	3.16	2.13	2.76	2.51	3.14	2.65	2.73	0.39
Complexus C ₃ –C ₄	0.80	0.67	0.72	0.64	1.04	0.55	0.74	0.17
Complexus C ₅	0.51	0.21	NM	0.20	0.40	0.28	0.32	0.13
Complexus C ₆	0.34	0.25	NM	0.28	0.36	0.37	0.32	0.05
Complexus C ₇	0.37	0.51	0.39	0.29	0.51	0.36	0.40	0.09
Complexus T ₁	0.49	0.30	0.49	0.38	NM	0.65	0.46	0.13
Sterno-occipitalis	0.52	0.43	0.33	0.49	0.48	0.54	0.47	0.08
Sternomastoideus	0.60	0.37	0.44	0.56	0.78	0.53	0.55	0.14
Sternohyoideus	0.12	0.24	0.12	0.18	0.26	0.43	0.22	0.12
Sternothyroideus	0.06	0.04	0.08	0.04	0.03	0.02	0.04	0.02
Scalenus supercostalis dorsalis	0.23	0.07	0.16	0.08	0.06	0.05	0.11	0.07
Scalenus supercostalis intermedius	0.11	0.21	0.10	0.19	0.23	0.09	0.15	0.06
Scalenus supercostalis ventralis	1.17	0.99	0.72	0.74	1.30	NM	0.98	0.26
Scalenus primae costae dorsalis	1.73	1.31	0.87	1.40	1.53	NM	1.37	0.32
Scalenus primae costae intermedius	0.92	0.86	0.80	0.77	0.97	NM	0.86	0.09
Scalenus primae costae ventralis	0.78	0.34	0.31	0.32	0.51	NM	0.45	0.20
Longus capitis C ₂	0.53	0.26	NM	0.53	0.51	NM	0.46	0.13
Longus capitis C ₂₋₃	0.59	0.79	0.54	0.34	0.39	NM	0.53	0.18
Longus capitis C ₄₋₅₋₆	1.08	1.04	0.83	0.80	1.18	NM	0.98	0.16
Longus colli C ₁ –C ₄	0.33	0.31	0.32	0.19	0.35	NM	0.30	0.06
Longus colli C ₂ –C ₅	0.32	0.32	0.36	0.34	0.47	NM	0.36	0.06
Longus colli C ₃ –C ₆	0.55	0.34	0.67	0.53	0.64	NM	0.55	0.13
Longus colli C ₆ –C ₇	0.11	0.19	0.18	0.25	0.17	NM	0.18	0.05
Longus colli C ₇ –T ₁	0.16	0.26	0.15	0.17	0.15	NM	0.18	0.05
Rectus capitis dorsalis Major	0.08	0.14	0.09	0.09	0.04	NM	0.09	0.03
Rectus capitis dorsalis Intermedius	0.40	0.35	0.23	0.29	0.39	NM	0.33	0.07
Rectus capitis dorsalis Minor	0.20	0.17	0.24	0.20	0.19	NM	0.20	0.03
Oblique capitis caudalis	1.98	1.50	1.54	1.34	1.84	NM	1.64	0.26
Oblique capitis carnialis principle	0.05	0.07	0.06	NM	0.05	NM	0.06	0.01
Oblique capitis carnialis accessory	0.04	NM	0.05	NM	0.03	NM	0.04	0.01

NM, not measured.

Table 5 Continued

(b) PCSA (cm)² as a fraction of body mass (kg)^{2/3}

Muscle	Subject						Mean	SD
	A	B	C	D	E	F		
Trapezius – cervical portion	0.80	0.56	0.50	0.57	0.44	0.41	0.55	0.14
Brachiocephalicus	0.70	0.63	0.49	0.45	0.37	0.35	0.50	0.14
Omotransversarius	0.43	0.33	0.32	0.33	0.24	0.19	0.31	0.08
Rhomboideus capitis	0.07	0.05	0.06	0.04	0.04	0.03	0.05	0.01
Rhomboideus cervicis	0.92	0.81	0.64	0.33	0.29	0.60	0.60	0.25
Serratus ventralis cervicis C ₂	NM	0.09	NM	0.07	0.02	0.12	0.07	0.03
Serratus ventralis cervicis C ₃	0.34	0.16	0.14	0.20	0.11	0.07	0.17	0.09
Serratus ventralis cervicis C ₄	0.24	0.19	0.18	0.11	0.10	0.09	0.15	0.06
Serratus ventralis cervicis C ₅	0.44	0.27	0.28	0.21	0.22	0.16	0.26	0.09
Serratus ventralis cervicis C ₆	0.31	0.24	0.33	0.19	0.31	0.20	0.26	0.06
Serratus ventralis cervicis C ₇	0.41	0.33	0.48	0.45	0.42	0.31	0.40	0.07
Splenius	1.47	1.17	0.88	1.00	0.99	0.86	1.06	0.23
Longissimus capitis	0.48	0.79	0.46	0.80	0.82	0.37	0.62	0.21
Longissimus cervicis C ₃	NM	0.07	0.06	0.08	0.09	0.21	0.10	0.06
Longissimus cervicis C ₄	NM	0.30	0.11	0.11	0.13	0.09	0.15	0.09
Longissimus cervicis C ₅	NM	0.18	0.18	0.10	0.35	0.06	0.18	0.11
Longissimus cervicis C ₆	NM	0.18	0.16	0.07	0.32	0.29	0.20	0.10
Spinalis et semispinalis	NM	0.26	0.21	0.34	0.25	0.22	0.26	0.05
Biventer cervicis	0.76	0.64	0.77	0.51	0.54	0.41	0.61	0.15
Complexus C ₃ –C ₄	NM	0.25	0.32	0.26	0.25	0.13	0.24	0.07
Complexus C ₅	NM	0.06	NM	0.06	0.09	0.06	0.07	0.01
Complexus C ₆	NM	0.07	NM	0.09	0.07	0.08	0.08	0.01
Complexus C ₇	NM	0.15	0.12	0.09	0.09	0.07	0.10	0.03
Complexus T ₁	NM	0.09	0.12	0.10	0.00	0.10	0.08	0.05
Sterno-occipitalis	0.16	0.14	0.11	0.16	0.10	0.10	0.13	0.03
Sternomastoideus	0.15	0.12	0.11	0.15	0.12	0.08	0.12	0.02
Sternohyoideus	0.06	0.12	0.06	0.07	0.08	0.17	0.10	0.04
Sternothyroideus	0.12	0.09	0.08	0.05	0.07	0.05	0.07	0.03
Scalenus supercostalis dorsalis	0.13	0.09	0.10	0.08	0.07	0.05	0.09	0.03
Scalenus supercostalis intermedius	0.07	0.12	0.06	0.10	0.11	0.06	0.09	0.03
Scalenus supercostalis ventralis	0.21	0.20	0.14	0.13	0.20	NM	0.17	0.04
Scalenus primae costae dorsalis	0.38	0.24	0.20	0.24	0.24	NM	0.26	0.07
Scalenus primae costae intermedius	0.23	0.17	0.13	0.13	0.15	NM	0.16	0.04
Scalenus primae costae ventralis	0.19	0.06	0.06	0.05	0.08	NM	0.09	0.06
Longus capitis C ₂	0.44	0.09	NM	0.29	0.30	NM	0.28	0.14
Longus capitis C ₂₋₃	0.31	0.52	0.20	0.16	0.17	NM	0.27	0.15
Longus capitis C ₄₋₅₋₆	0.47	0.26	0.31	0.22	0.35	NM	0.32	0.10
Longus colli C ₁ –C ₄	0.42	0.43	0.37	0.28	0.41	NM	0.38	0.06
Longus colli C ₂ –C ₅	0.44	0.40	0.49	0.53	0.54	NM	0.48	0.06
Longus colli C ₃ –C ₆	NM	0.35	0.87	0.59	0.69	NM	0.63	0.21
Longus colli C ₆ –C ₇	NM	0.35	0.33	0.30	0.25	NM	0.31	0.04
Longus colli C ₇ –T ₁	NM	0.48	0.24	0.23	0.23	NM	0.30	0.12
Rectus capitis dorsalis Major	0.16	0.16	0.15	0.19	0.09	NM	0.15	0.04
Rectus capitis dorsalis Intermedius	0.47	0.47	0.25	0.27	0.57	NM	0.41	0.14
Rectus capitis dorsalis Minor	0.22	0.22	0.29	0.22	0.23	NM	0.23	0.03
Oblique capitis caudalis	1.41	0.74	0.97	0.80	0.95	NM	0.98	0.26
Oblique capitis carnialis principle	0.08	0.09	0.09	NM	0.06	NM	0.08	0.01
Oblique capitis carnialis accessory	0.04	NM	0.08	NM	0.04	NM	0.05	0.02

NM, not measured.

Table 5 Continued

(c) Fascicle length (cm) as a fraction of body mass (kg)^{1/3}

Muscle	Subject						Mean	SD
	A	B	C	D	E	F		
Trapezius – cervical portion	1.95	2.15	2.21	1.99	2.77	2.43	2.25	0.31
Brachiocephalicus	6.33	5.90	7.34	7.77	9.65	8.56	7.59	1.40
Omotransversarius	3.86	4.54	4.53	4.35	6.77	5.91	4.99	1.10
Rhomboideus capitis	4.24	4.66	4.40	4.77	6.43	6.57	5.18	1.04
Rhomboideus cervicis	1.49	1.46	1.76	2.40	3.01	2.10	2.04	0.60
Serratus ventralis cervicis C ₂	NM	2.32	NM	3.21	5.07	5.15	3.94	1.40
Serratus ventralis cervicis C ₃	2.94	2.72	2.30	3.05	4.29	4.54	3.31	0.90
Serratus ventralis cervicis C ₄	2.75	2.11	2.42	2.76	3.54	3.98	2.93	0.70
Serratus ventralis cervicis C ₅	2.34	2.00	2.21	2.91	2.98	3.70	2.69	0.63
Serratus ventralis cervicis C ₆	2.10	2.00	1.62	2.07	1.90	2.81	2.08	0.40
Serratus ventralis cervicis C ₇	1.75	1.28	1.24	1.59	1.43	1.82	1.52	0.24
Splenius	3.12	3.30	3.04	3.69	3.88	4.35	3.56	0.50
Longissimus capitis	1.99	1.13	1.22	1.17	1.24	2.98	1.62	0.74
Longissimus cervicis C ₃	NM	2.93	2.72	3.66	4.12	2.15	3.12	0.78
Longissimus cervicis C ₄	NM	1.30	2.84	2.86	3.47	4.18	2.93	1.06
Longissimus cervicis C ₅	NM	2.28	2.19	2.81	1.81	3.28	2.47	0.57
Longissimus cervicis C ₆	NM	1.78	1.84	3.27	1.75	1.86	2.10	0.66
Spinalis et semispinalis	NM	3.80	5.47	4.40	6.38	4.99	5.01	0.99
Biventer cervicis	3.92	3.12	3.38	4.65	5.50	6.09	4.44	1.19
Complexus C ₃ –C ₄	NM	2.51	2.12	2.34	3.97	3.89	2.97	0.89
Complexus C ₅	NM	3.36	NM	2.98	4.33	4.36	3.76	0.69
Complexus C ₆	NM	3.26	NM	3.00	4.99	4.61	3.96	0.98
Complexus C ₇	NM	3.12	3.06	3.11	5.25	5.15	3.94	1.15
Complexus T ₁	NM	2.96	3.86	3.61	NM	5.88	4.08	1.26
Sterno-occipitalis	3.01	2.89	2.99	3.00	4.62	4.91	3.57	0.93
Sternomastoideus	3.78	2.83	3.73	3.60	5.93	5.94	4.30	1.31
Sternohyoideus	1.71	1.87	1.93	2.30	3.05	2.33	2.20	0.48
Sternothyroideus	0.50	0.39	0.89	0.72	0.42	0.43	0.56	0.20
Scalenus supercostalis dorsalis	1.68	0.75	1.45	0.94	0.78	0.96	1.09	0.38
Scalenus supercostalis intermedius	1.54	1.58	1.66	1.81	1.93	1.47	1.66	0.17
Scalenus supercostalis ventralis	5.37	4.73	4.85	5.56	6.08	NM	5.32	0.55
Scalenus primae costae dorsalis	4.31	5.18	4.12	5.58	6.07	NM	5.05	0.83
Scalenus primae costae intermedius	3.76	4.78	5.81	5.75	6.12	NM	5.24	0.97
Scalenus primae costae ventralis	3.80	5.36	5.04	6.28	5.77	NM	5.25	0.94
Longus capitis C ₂	1.15	2.58	NM	1.76	1.59	NM	1.77	0.60
Longus capitis C ₂₋₃	1.80	1.42	2.53	2.01	2.15	NM	1.98	0.41
Longus capitis C ₄₋₅₋₆	2.15	3.84	2.48	3.39	3.16	NM	3.01	0.68
Longus colli C ₁ –C ₄	0.74	0.69	0.82	0.64	0.80	NM	0.74	0.08
Longus colli C ₂ –C ₅	0.68	0.75	0.69	0.60	0.82	NM	0.71	0.08
Longus colli C ₃ –C ₆	NM	0.92	0.73	0.85	0.87	NM	0.84	0.08
Longus colli C ₆ –C ₇	NM	0.52	0.51	0.78	0.65	NM	0.62	0.13
Longus colli C ₇ vT ₁	NM	0.52	0.58	0.68	0.60	NM	0.60	0.07
Rectus capitis dorsalis Major	0.44	0.80	0.54	0.43	0.48	NM	0.54	0.15
Rectus capitis dorsalis Intermedius	0.80	0.69	0.88	0.99	0.65	NM	0.80	0.14
Rectus capitis dorsalis Minor	0.85	0.73	0.79	0.88	0.80	NM	0.81	0.06
Oblique capitis caudalis	1.33	1.91	1.49	1.57	1.82	NM	1.62	0.24
Oblique capitis carnialis principle	0.65	0.73	0.65	NM	0.69	NM	0.68	0.04
Oblique capitis carnialis accessory	0.82	NM	0.69	NM	0.64	NM	0.72	0.09

NM, not measured.

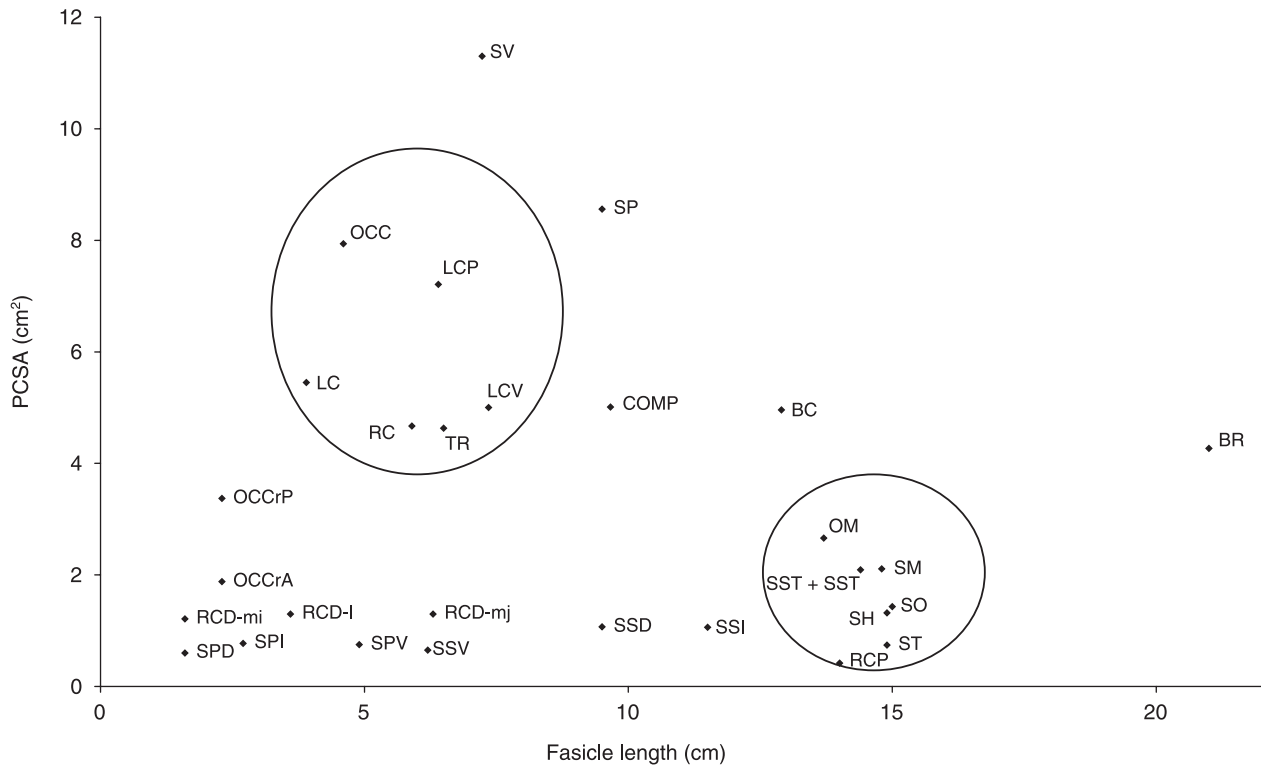


Fig. 3 Scatter graph of fascicle length and PCSA of the neck musculature of the dog. Groups of muscles characterized by long fascicle–small PCSA and short fascicle–large PCSA are surrounded by circles. Muscle abbreviations: TR, trapezius – cervical portion; OM, omotransversarius; RC, rhomboideus cervicis; RCP, rhomboideus capitis; SV, serratus ventralis cervicis; BR, brachiocephalicus; LC, longissimus capitis; BC, biventer cervicis; COMP, complexus; LCV, longissimus cervicis; SSC, spinalis et semispinalis cervicis; SST, spinalis et semispinalis thoracis; SO, sterno-occipitalis; SM, sternomastoideus; SH, sternohyoideus; ST, sternothyroideus; SSD, scalenus supracostalis dorsal division; SSI, scalenus supracostalis intermediate division; SSV, scalenus supracostalis ventral division; SPD, scalenus primae costae dorsal division; SPI, scalenus primae costae intermediate division; SPV, scalenus primae costae ventral division; LCP, longus capitis; RCD.mj, rectus capitis dorsalis major; RCD.i, rectus capitis dorsalis intermedius; RCD.mi, rectus capitis dorsalis minor; OCC, oblique capitis caudalis; OCCr.P, oblique capitis cranialis principle part; OCCr.A, oblique capitis cranialis accessory part.

In order to evaluate interobserver effects on the results obtained for total muscle length and fascicle length, parameters were measured by two independent observers (J.M. and A.S.). Differences were found to be less than 2%.

For the sake of brevity, throughout the remainder of the text cervical and thoracic vertebrae will be denoted by the letter 'C' and 'T', respectively, followed by a subscript to denote the position of the vertebra (i.e. C₆ for the 6th cervical vertebrae).

Muscles originating on the vertebral column and inserting on the shoulder girdle

Trapezius (TR). The cervical and thoracic portions of the TR were separated along the tendinous band that ran between the two parts of the muscle. This separa-

tion ran dorsally from the spine of the scapula to the median raphe of the neck. In dogs A and C the tendinous band was not clearly defined, and the muscle was separated along a line extending dorsally from the spine of the scapula to the median raphe of the neck adjacent to the spinous process of T₂. The muscle fascicles of the TR originated on the midline between C₃ and T₂, and coursed at angles ranging from 0° to 12° with respect to the line connecting their origin and insertion sites. At the cranial and caudal extremes of their vertebral origin, the fascicles were attached directly to the median raphe of the neck. At the centre of its vertebral origin (C₄–C₇), the muscle was attached to the midline by an aponeurotic sheet. Fascicles were longest at the cranial end of the muscle, and became progressively shorter and less steeply angled toward the tendinous band (Fig. 4a).

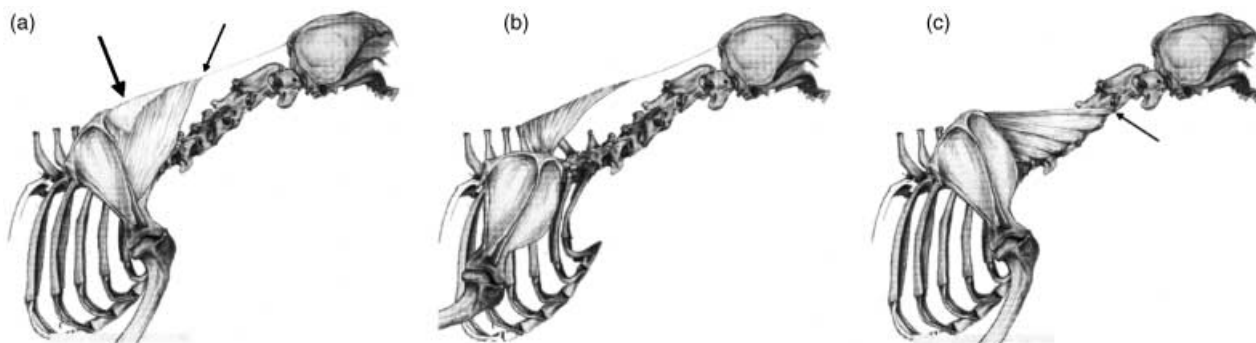


Fig. 4 Schematic drawing illustrating the anatomical relationships of muscles originating from the cervical vertebrae and inserting on the shoulder girdle. (a) The trapezius (TR) is attached to the midline by an aponeurotic sheet at the centre of its vertebral origin (C_4 – C_7) (Large arrow). Fascicles are longest at the cranial end of the muscle (small arrow), and become progressively shorter and less angled toward the tendinous band. (b) The cervical portion of the rhomboideus cervicis (RC) is separated from the thoracic portion along a line extending dorsally from the scapular spine. Its fascicles are longest at the cranial end, and become shorter and progressively less angled caudally. (c) The cervical portion of the serratus ventralis (SV) in four dogs had an additional division, which originated cranially on the facies serrata and inserted on the transverse process of C_2 (arrow).

Omotransversarius (OM). This muscle originated on the caudal aspect of the wing of the atlas and inserted on the distal portion of scapular spine. In one dog (D), the site of origin included also the fascia covering the intertransversarius.

Rhomboideus cervicis (RC). This muscle was separated from its thoracic counterpart (rhomboideus thoracis) by a line which extended dorsally from the scapular spine. Similar to the TR, the fascicles of the RC were long and steeply angled at the cranial end, and became shorter and progressively less angled toward the caudal end (Fig. 4b).

Serratus ventralis cervicis (SV). This muscle comprised five clearly defined divisions, each inserting on a different vertebra (C_3 – C_7). In dogs B and D–F the muscle had an additional division, which originated cranially on the facies serrata and inserted on the transverse process of C_2 (Fig. 4c, SV with six divisions). The two caudal divisions were more highly pinnate so that their fascicle lengths were shorter, and their PCSA was therefore larger as compared with the other divisions (Table 3).

Muscles originating on the shoulder girdle and inserting on the skull

Brachiocephalicus (BR). This muscle was divided into two subunits; cleidomastoideus (CM), which inserted on the mastoid process of the temporal bone, and cleidocervicalis (CC), which inserts on the fibrous raphe of the cranial half of the neck (Fig. 5).

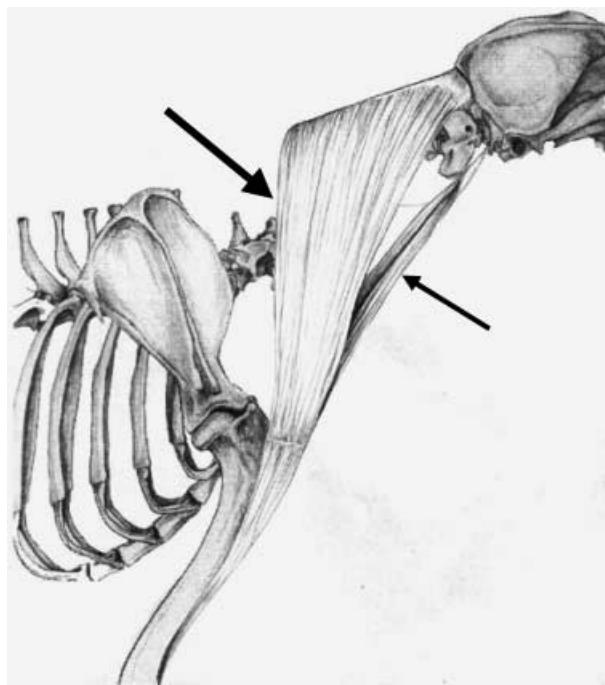
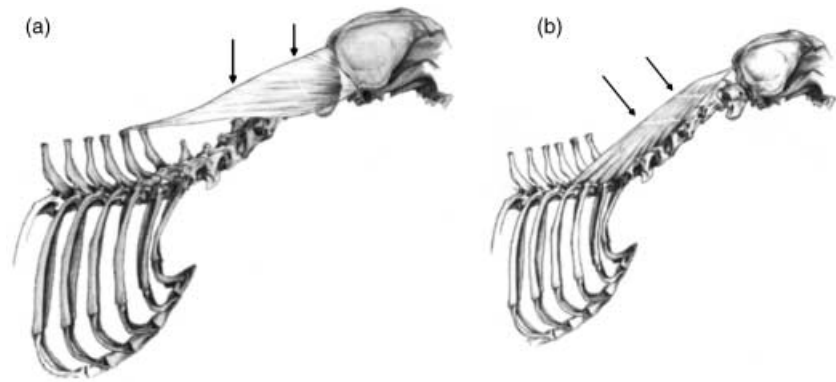


Fig. 5 Schematic drawing illustrating the anatomical relationships and organization of the two heads of brachiocephalicus: the cleidomastoideus (CM), which inserts on the deep-mastoid part of temporal bone (small arrow), and the cleidocervicalis (CC), which inserts on the fibrous raphe of the cranial half of the neck (large arrow).

The CM portion was heavier than the CC portion, and its fascicles were shorter. As a result, it had a larger PCSA when compared with the CC (PCSA values of 2.25 and 2.03 cm^2 , respectively).

Fig. 6 Schematic drawing illustrating the structural features of muscles that originate on the vertebral column and insert on the skull. (a) The line drawing of splenius (SP) shows its triangular appearance. Two tendinous inscriptions, which run perpendicular to the fascicle's direction, extend to about half the muscle's thickness (arrows). (b) The line drawing of longissimus capitis (LC) shows the tendinous inscriptions (arrows) which divide LC into three parts.



In all dogs, a few muscle fascicles were observed connecting the CC and CM portions of BR. In dog C, the CM was found to have two muscle bellies, which inserted separately on the mastoid part of the temporal bone.

Rhomboideus capitis (RCP). This muscle originated on the dorso-cranial border of scapula, and inserted on the nuchal crest. Its PCSA was found to be relatively small (a PCSA value of less than 0.65 cm² in all dogs).

Muscles originating on the vertebral column and inserting on the skull

Splenius (SP). This large, flat and triangular muscle was positioned between the third thoracic vertebra and the skull. Its fascicles ran in a cranio-ventral direction (Fig. 6a). The SP was incompletely divided into three by two tendinous inscriptions, which ran perpendicular to the direction of the muscle fascicles. The architecture of the fascicles was found to be different in superficial and deep aspects of the muscle, due to the incomplete nature of these inscriptions. Fascicles ran uninterrupted from origin to insertion in the deep aspect, whereas in the superficial aspect, fascicles were divided by tendinous inscriptions and as a result were much shorter.

Longissimus capitis (LC). This muscle was completely divided into two (dogs A and F) or three (dogs B–E) subdivisions by tendinous inscriptions running perpendicular to the direction of its muscle fascicles (Fig. 6b). The insertion of this muscle by means of a single tendon on the mastoid part of the temporal bone was noted in all dogs except dog E, where two tendons of insertion (to the same point) were found.

Biventer cervicis (BC). Oblique tendinous inscriptions divided this muscle into five (dogs A–C, E and F) or six

divisions (dog C). Cranially the tendinous inscriptions completely bisected the cranio-caudally orientated muscle fascicles. Caudally, the muscle was incompletely divided, and thus exhibited a wide variety of muscle fascicle lengths (Fig. 7a). Longer fascicles were found passing through tendinous inscriptions in areas where the tendinous inscriptions were incomplete (Fig. 7b).

Complexus (COMP). This muscle originated on the caudal articular processes of vertebrae C₃ to T₁ and inserted on the dorsal nuchal line. Divisions within this muscle varied between dogs. The two parts which originated on the articular processes of C₃ and C₄ could not be easily separated in all dogs (Fig. 7c), and were therefore considered as one segment (C₃₋₄). In dog E the COMP was not attached to the articular process of T₁. In dog C it was not possible to separate the four cranial parts (C₃–C₄–C₅–C₆) and they were therefore considered to be one segment (C₃₋₄₋₅₋₆).

Muscles with their origin and insertion on the vertebral column

Longissimus cervicis (LCV). This muscle consisted of four distinct divisions, all of which originated on the articular processes of T₁ to T₆ and on the spinous process of T₆. Each division inserted consecutively on the transverse processes of C₃ to C₆ (Fig. 8a).

Spinalis et semispinalis thoracis (SST). This muscle extended from the last two cervical vertebrae to the caudal part of the thoracic spine. Only the two divisions that inserted on C₆ and C₇ were considered in this study (Fig. 8b).

Spinalis et semispinalis cervicis (SSC). This muscle arose from the spinous process of T₁ and inserts via four tendinous inscriptions on the spinous processes of C₅ to C₂ (Fig. 8b).

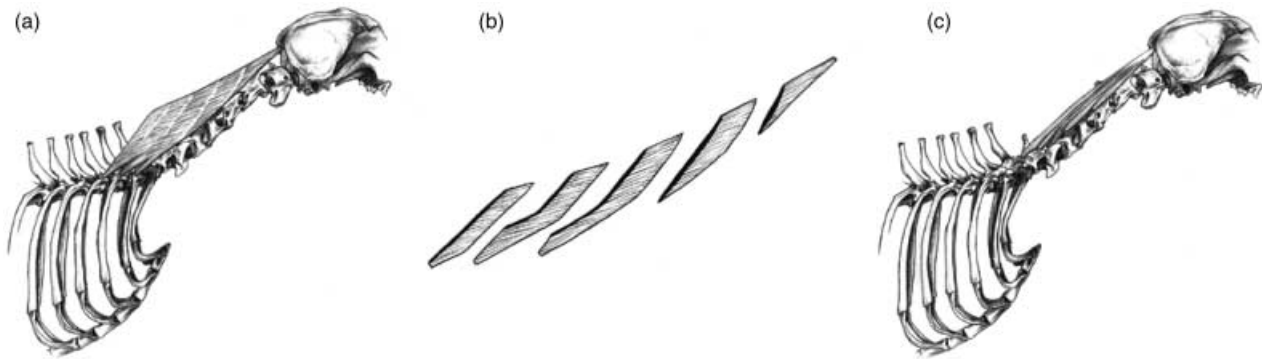


Fig. 7 Schematic drawing illustrating the structural features of muscles that originate on the vertebral column and insert on the skull. (a) The line drawing of biventer cervicis (BC) shows its compartmentalized structure due to its tendinous inscriptions, which cross the muscle fascicles obliquely, and divide this muscle into five divisions. (b) An exploded view of BC when compartments are separated from one another along the tendinous inscriptions. Unlike the simple structure of the cranial compartments, the caudal compartments have a more complex organization, with a wide variety of fascicle lengths coexisting within them. (c) The organization of muscle heads of complexus (COMP) demonstrates that the two heads, which originate from the articular processes of C_3 and C_4 , could not be easily separated in all dogs.

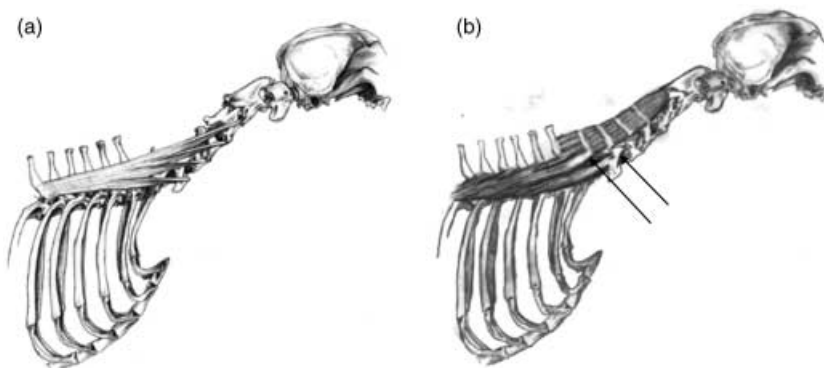


Fig. 8 This schematic drawing illustrates the structural features of muscles with their origin and insertion on the vertebral column. (a) All divisions of the longissimus cervicis (LCV) originate from the articular processes of T_1 to T_6 and from the spinous process of T_6 . Each division inserts on a different transverse process, from C_3 to C_6 . (b) Only the two serrations of spinales et semispinales thoracis (ST) and cervicis (SC) that insert on the sixth and seventh cervical vertebra were considered in this study (arrows). SC inserts via four tendinous inscriptions on the spinous processes of the second to the fifth cervical vertebra.

Multifidus cervicis (MC). The MC ran obliquely between the articular processes of the lower cervical vertebrae and the spinous processes of the more cranial vertebrae. The MC consisted of six incompletely separable divisions, which were further divided into superficial and deep divisions.

Intertransversarii cervicis (IC). The IC ran from the first thoracic to the second cervical vertebrae. It consisted of three groups of fascicle lengths reflecting different muscles strands connecting diverse points on the cervical vertebrae (e.g. transverse processes to articular processes, or caudal articular processes to cranial processes of the preceding vertebrae).

The method of PCSA calculation was considered unreliable for MC and IC due to their complex architecture, and is thus not included in the reported results.

Muscles originating on the rib cage and inserting on the vertebral column

Sternocephalicus. This muscle consisted of two divisions which shared a common origin on the manubrium sterni: sterno-occipitalis (SO) and sternomastoideus (SM). The SM was thicker than the SO, and although both muscles were found to have similar mean fascicle lengths, SM was found to have a larger PCSA (values of 2.11 and 1.43 cm^2 , respectively).

Sternohyoideus (SH). This muscle originated on the manubrium sterni and inserted on the basihyoid bone.

Sternothyroideus (ST). This muscle originated on the first costal cartilage and inserted on the thyroid cartilage. ST had a smaller PCSA than SH (values of 0.74 and 1.32 cm^2 , respectively).

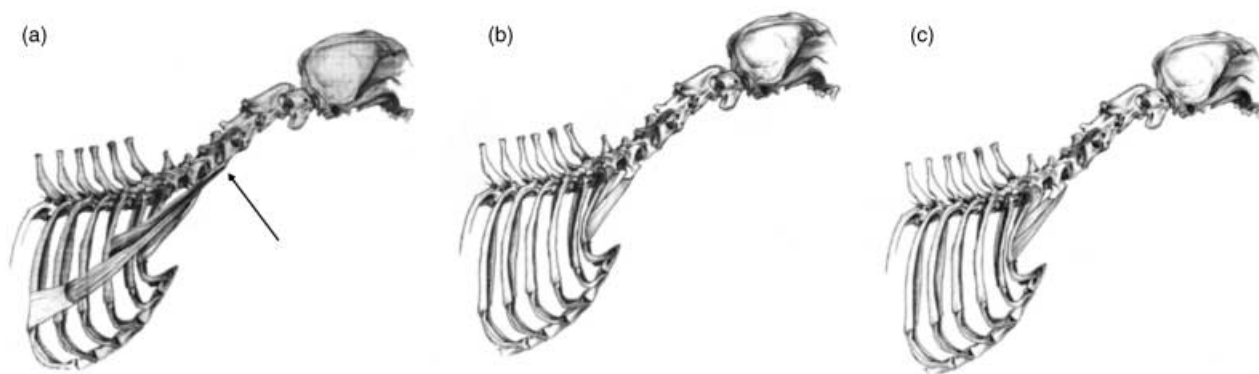


Fig. 9 Schematic drawing illustrating the structural features of muscles that originate on the ribs and insert on the vertebral column. (a) Three distinct divisions of the scalenus supracoastalis (SS) insert on the caudal aspect of the transverse processes of C₄ and C₅ by means of two tendons. (b) The insertion site of the intermediate division of the scalenus primae costae (SPI) was found to be C₆ in some dogs, whereas in other dogs it was C₇. (c).

Scalenus supracoastalis (SS). This muscle consisted of three distinct divisions which inserted on the caudal aspect of the transverse processes of C₄ and C₅ by means of two tendons (Fig. 9a).

Dorsal division (SSD). In dogs A and C the SSD originated on the upper third of the fourth rib, in dogs B, D and F it originated on the third and fourth ribs, and in dog E on the third rib only.

Intermediate division (SSI). This division originated on the middle part of the sixth, seventh and eighth ribs, by means of an aponeurotic sheet and directly by a muscular origin on the fifth rib. In dog A, a muscular attachment to the fourth rib was also present.

Ventral division (SSV). This division originated directly on the lower third of the first rib. This division was considered as part of the SS muscle due to its common tendons of insertion. SSV was smaller and thinner than the other two divisions of the muscle and consequently has a lower PCSA value.

Scalenus primae costae (SP). In all dogs this muscle could be partitioned into three divisions. All of these originated on the first rib and inserted on C₆ or C₇ (Fig. 9b).

Dorsal division (SPD). In all dogs this division was found to insert on the transverse process of C₇, forming a triangle between C₇ and the tubercle of the first rib.

Intermediate division (SPI). In dogs A, C and F this division was found to insert on the caudal part of the transverse process of C₆, whereas in dogs B, D and E it inserted on the transverse process of C₇.

Ventral division (SPV). This inserted on the cranial part of the transverse process of C₆.

Ventral muscles

Longus capitis (LCP). This complex muscle was divided into three parts. The muscle originated on the transverse processes of C₆ to C₂, and inserted on the muscular tubercle of the basioccipital bone, between the tympanic bullae. The rostral division originated on the cranial aspect of the transverse process of C₂; the second division originated on the caudal aspect of the transverse process of C₂ and the cranial aspect of the transverse process of C₃; the third division originated on the transverse processes of C₄, C₅ and C₆. In one dog (C), the rostral and second divisions could not be clearly separated.

Longus colli (LCO). Only those bundles of the LCO with their origin or insertion sites on the cervical spine were included in the dissection. They consisted of a cervical part and a cranial thoracic part.

Cervical part – this part consisted of three divisions, which coursed cranio-medially. Each arose on the ventral border of its respective cervical transverse process, namely the sixth, fifth and fourth cervical vertebra. Each division passed over two vertebrae and ended on the ventral spine of the third to the first cervical vertebrae.

Thoracic part – this part consisted of two divisions, both orientated cranio-laterally. The first division originated on the ventral body of T₁ and inserted on the transverse process of C₇, and the second division originated on the ventral body of C₇ and inserted on the transverse process of C₆.

Rectus capitis lateralis (RCL) and rectus capitis ventralis (RCV). These small muscles were difficult to dissect. RCL could not be found in one dog (D), and RCV could not be found in two dogs (B and D). Both RCL and

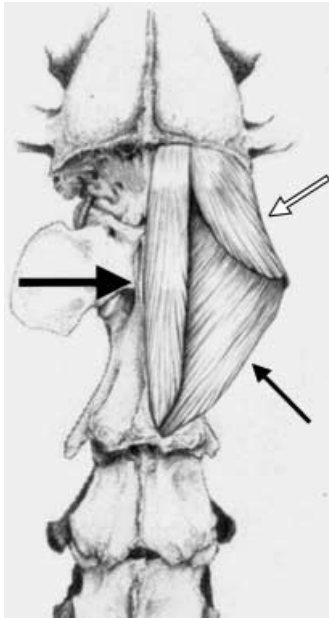


Fig. 10 Schematic drawing of muscles that connect the cranial cervical vertebrae and the skull. Rectus capitis dorsalis (large arrow), oblique capitis caudalis (small arrow) and oblique capitis cranialis (open arrow).

RCV had a particularly non-uniform organization, and thus only an estimate of their morphometric parameters is provided (see Table 2).

Sub-occipital muscles

The first two cervical vertebrae were invested with three groups of short muscles that cover all surfaces of the axis and atlas (Fig. 10).

Rectus capitis dorsalis (RCD). This muscle was composed of three parts that traverse the dorsal aspect of the upper cervical spine and attach along the entire length of the nuchal line. The three parts were arranged from deep to superficial; the most superficial part, RCD major, originated on the caudal end of the axis; the intermediate part, RCD intermedius, originated on the cranial end of the axis; and the deep part, RCD minor, originated on the atlas. Although the three parts varied in their lengths due to their different points of origin, the effect on PCSA values was minimal (see Table 3).

Oblique capitis caudalis (OCC). This muscle originated on the entire spinous process of the axis, and inserted on the wing of the atlas. The OCC was distinguished by its relatively large weight combined with relatively short fascicles; therefore, its PCSA was large (a value of 7.94 cm²).

Oblique capitis cranialis (OCCr). This muscle consisted of two distinct parts, the principal part (OCCrP) and the accessory part (OCCrA). The OCCrP originated on the lateral border of the wing of the atlas and inserted on the mastoid part of the temporal bone. The OCCrA originated on the tip of the wing of the atlas and inserted on the dorsal nuchal line. As the names imply, the OCCrP had a larger PCSA than the OCCrA (values of 3.37 and 1.88 cm², respectively).

Discussion

Thorough knowledge of the internal organization of the cervical musculature, its architecture and the various functions of the different muscles are essential for interpretation of the design and function of the neck in any mammal (Gellman et al. 2002). This study provides a systematic description of the anatomy and morphometry of the musculature of the canine neck. These data will serve as a foundation for future analyses of canine cervical spine mechanics, and are crucial for interpretation of the results of studies utilizing the canine cervical spine as a model for the human neck.

Although several elegant studies (e.g. Tsuang et al. 1993; Stokes & Gardner-Morse, 1999) investigated the morphometry of limb musculature in various species by advanced imaging modalities, the complex anatomy of the musculature of the neck renders these techniques ineffective for this body segment. This is due to the fact that non-invasive imaging techniques such as magnetic resonance imaging (MRI) and computed tomography (CT) are limited in their resolution of muscle architecture (Veeger et al. 1991; Kamibayashi & Richmond, 1998; Lieber & Friden, 2000; Delp et al. 2001). In addition, these methods are not suitable for muscles which have more than one compartment or multiple lines of action, as occurs in many neck muscles (Friederich & Brand, 1990; Engstrom et al. 1991; Richmond, 1998).

Accuracy of the determination of muscle properties

PCSA was calculated based on the measured values of muscle mass, fascicle length and pennation angle, according to Eq. (1). This approach has previously been employed in studies of neck muscles in humans (Kamibayashi & Richmond, 1998), non-human primates (Cheng & Scott, 2000; Richmond et al. 2001) and felids (Selbie et al. 1993; Richmond et al. 1999). The muscles

of the canine neck are complex due to their multiple attachments to different vertebrae and other bones, varied lengths of fascicles, and multiple tendinous inscriptions. Such architectural complexity impacts on the accuracy of PCSA determination. The validity of the information represented by PCSA depends therefore on the accuracy of the measurements and on the precise description of architectural geometry (Otten, 1988; Richmond, 1998).

In this report, architecturally complex muscles were divided according to anatomical observations. This method has been shown to increase the validity of the morphometric data obtained significantly (Van der Helm & Veenbaas, 1991; Johnson et al. 1996; Klein Breteler et al. 1999). The mass, fascicle length, PCSA and AI of each division were calculated individually. Divisions of muscles with broad attachment sites have been previously described in studies of muscles of the shoulder region (Dumas et al. 1991; Van der Helm & Veenbaas, 1991; Johnson et al. 1996), human neck muscles (Kamibayashi & Richmond, 1998) and the canine forelimb (Shahar & Milgram, 2005). The division of a complex muscle into its constituent parts had a significant impact on calculated PCSA values. For example, the PCSA of the undivided LCP has a value of 4.5 cm² and the sum of the PCSAs of the divisions of the LCP has a value of 7.21 cm². This difference clearly affects the predicted forces generated by this muscle. It should be noted that the mean PCSA of each muscle was chosen to be the average of the PCSA values of the six dogs, and therefore will not necessarily correspond to a value obtained by using 'mean' mass and 'mean' fascicle length in Eq. (1).

Previous reports (Vasavada et al. 1996; Kamibayashi & Richmond, 1998) have shown that a measured fascicle length is dependent on head–neck position during rigor mortis, reflecting different degrees of actin–myosin overlap. In this study, specimens were dissected immediately following euthanasia, as opposed to dissection of embalmed cadavers, and thus the entire dissection process was completed within 5–7 h from the time of death; as a result rigor mortis had only a minor effect on fascicle length measurements. Another advantage of fresh cadaver dissection was the fact that all muscles comprising the canine neck could be studied, including those which adhere closely to the vertebrae and were consequently ignored in previous studies (Kamibayashi & Richmond, 1998; Richmond et al. 1999, 2001). Moreover, gathering muscle parameters

before the occurrence of tissue desiccation allowed a more accurate measurement of muscle mass, and thus a more reliable estimate of the PCSA.

The division of complex muscles into parts was based on anatomical criteria alone. Divisions based on functional criteria would be more valid physiologically. Such an approach requires knowledge of the innervation patterns and recruitment strategies of the different muscle divisions during motor activity, which are currently unavailable.

Multifidus cervicis and intertransversarii cervicis were difficult to characterize. This was due to the fact that these muscles were architecturally complex and closely adhered to the vertebrae. Other researchers have faced similar problems, and have stated that these muscles are so complex that they defy analysis by dissection (Kamibayashi & Richmond, 1998; Richmond et al. 1999, 2001). Because of the strategic position and the relatively large mass of the multifidus cervicis and intertransversarii cervicis, we believe that these muscles make a fundamental contribution to canine neck dynamics, and thus we present their basic data, which consists of mass and total length (see Table 2).

Inter- and intra-individual variation of muscle properties

Some muscles of the canine cervical spine were found to have a rather large range of inter-individual variability in their anatomical divisions, attachment sites and the number of tendinous inscriptions crossing them. For example, the complexus was found to have five divisions in some dogs, but only four or even three divisions in others (Fig. 7c). Similarly, the insertion site of the intermediate division of the scalenus prima costae (SPI) was found to be C₆ in some of the dogs, whereas in the others it was C₇ (Fig. 9b,c). However, this variability did not seem to have major functional significance, and for most muscles inter-individual variability was found to be low.

Bilateral dissection was undertaken in one dog, and revealed only subtle differences between the right and left side of the same dog in features such as the attachment site of the dorsal division of the scalenus superficialis (SSD); the right SSD originated from the upper third of the third and fourth ribs, whereas the left SSD originated only from the fourth rib. The similarity of results for all muscle pairs in the bilateral dissection, after normalization of fascicle lengths to a standard

sarcomere length (see Table 4), confirmed dissection precision, demonstrated the consistency of the method of dividing muscles and supported the assumption that the musculature of the canine neck is approximately symmetrically constructed.

Muscle mass, PCSA and fascicle lengths were scaled by body mass (assuming geometric similarity) in order to allow comparison between dogs of different sizes. The scaled values of PCSA, fascicle length and muscle mass were found to be quite similar (Table 5a–c) for all dogs of this study. In some muscles PCSA magnitude did not correlate with body mass. For example, *romboideus cervicis* had a PCSA value of 4.56 cm² in dog D (body mass 20 kg), whereas the same muscle had a PCSA value of 2.65 cm² in dog C, which was much heavier (body mass 27 kg). Similar variability has been observed in humans (Kamibayashi & Richmond, 1998), horses (Payne et al. 2005a,b) and felids (Richmond et al. 1999). Hence, in addition to reporting the mean values of the measured parameters, information about the range of variation found is also provided in Tables 2–4. On visual inspection, dog A seemed particularly well muscled and the scaled PCSA values of 21 of the 48 muscles studied were substantially larger than those of the other dogs.

Differences between findings presented here and textbooks descriptions

Most of the anatomical descriptions presented here concur with data previously reported in veterinary anatomical textbooks (e.g. Nickel et al. 1986; Evans & Christensen, 1993). In several instances, however, our findings varied substantially from those described in the textbooks. Some noteworthy examples include the existence of an additional C₂ division of the *serratus ventralis* in some dogs, which has not previously been reported; the cervical part of the *longus colli*, which contains only three divisions (instead of the previously described four), each passing over two vertebrae (instead of one); and the origin of the *longissimus capitis* on the articular processes (and not the transverse processes) of T₁–T₃ vertebrae. These variations did not, however, seem to have substantial functional significance.

Comparative morphometry

When comparing the morphometry of the canine and human cervical musculature, it is important to keep in

mind two significant differences of skeletal configuration between these species. In the dog, as in other quadruped mammals, the centre of mass of the head and neck is located in front of the vertebral column and active muscle contraction is required to support its weight. By contrast, the human head is carried more directly over the trunk, so that much of its weight is borne passively (Tobias 1992; Graf et al. 1995; Richmond et al. 2001). Therefore, caution should be exercised when trying to extrapolate the function of muscles from the similarities in location between them in these two species. Thus, muscles involved with maintenance of head position in canines, such as the *rectus capitus dorsalis* and *splenius*, have higher PCSAs when compared with the equivalent muscles in humans. This is clearly shown in Fig. 2, where all muscles except the *trapezius* can be seen to have PCSA values (after scaling) that are substantially higher in dogs than those of the equivalent muscles in humans. The *trapezius* is of special interest because although it plays a role in forelimb weight bearing, its PCSA value in the dog is lower than in humans. This may be due to the fact that in humans the *trapezius* is involved in both the stabilization of the shoulder and the control of grasping motions; dogs, by contrast, are unable to perform grasping motions with their forelimbs, and therefore this muscle serves only to stabilize their forelimb and is less well developed.

In addition, the front limb of the dog participates in locomotion and weight bearing, whereas the main function of the equivalent human limb is object manipulation. This difference is manifested by the specialized morphology and orientation of the human limb. For example, the scapula of the dog is orientated in the sagittal plane, whereas in humans the scapula lies in the frontal plane; in the dog only a remnant of the clavicle exists, as compared with the fully developed human clavicle. As a result, differences exist in the architectural organization of some muscles, and the location of their attachments to the shoulder girdle is different.

Other canine characteristics, such as the absence of a clavicle and the participation of the forelimb in weight bearing, also impact on the neck musculature. For example, the cervical part of the *serratus ventralis* is one of the main stabilizers of the scapula and plays an important role in weight bearing; therefore, its PCSA value in the dog is much higher than in humans. The same applies to the *rhomboideus* and the *brachiocephalicus*, two other extrinsic muscles of the canine forelimb that contribute to weight bearing.

Comparative anatomy

There are several neck muscles in the dog whose origins and insertions resemble those of humans, but their nomenclature differs (Gray, 1980; Richmond & Vidal, 1990). The canine serratus ventralis is analogous to the human levator scapulae ventralis and the canine rhomboideus cervicis is analogous to the human rhomboideus minor. Other variations in nomenclature are explained by the differences in orientation of various body segments in these species; thus, dorsal muscles in the dog are posterior muscles in humans and similarly ventral muscles in the dog are inferior muscles in humans, e.g. the rectus capitis dorsalis of the dog is equivalent to the rectus capitis posterior in humans. Additionally, several muscles of the canine neck, such as the omotransversarius and rhomboideus capitis, have no analogous human muscle. The converse is also true, with muscles such as the atlantoscapularis and splenius cervicis absent in the dog. Nevertheless, most neck muscles in dogs and humans are similar in both their internal design and their general architecture.

The data obtained in this study allowed us to examine the significance of the relationship between PCSA–fascicle length and muscle function in the dog. In particular we examined muscle groups that are characterized by long fascicles–small PCSA, and vice versa. For example, muscles which run between the cranial neck and the rib cage (e.g. sterno-occipitalis, sternomastoideus) or the shoulder girdle (e.g. omotransversarius and rhomboideus capitis) are characterized by their relatively long fascicles and low PCSA values and appear to be designed for large excursions (Fig. 3); specifically, note the extremely long fascicles and low PCSA of the brachiocephalicus. By contrast, muscles that support the neck and shoulder against gravitational forces (e.g. serratus ventralis, trapezius, and rhomboideus cervicis) have relatively high PCSA values combined with short fascicle length, and thus appear to be suited for generating large forces (Fig. 3).

The findings reported in this study can be used to examine the suitability of using the dog as a model for the human cervical spine. In general, most canine cervical muscles were found to have homologous human muscles; furthermore, their scaled morphometric properties were seen to be similar. Although in a few instances differences were found in either the anatomy or the morphometry of certain muscles, and major differences in the range of motion of the various articulations

of the head and neck were previously reported (Graf et al. 1995), similarities were the rule rather than the exception. The total range of motion at the cervicothoracic junction has been shown to be similar in all vertebrates (Graf et al. 1995). Comparison of our results with those of Kamibayashi & Richmond (1998) demonstrates that in both dog and humans homologous neck muscles have high PCSA values and are adapted to force generation (with the exception of serratus ventralis and trapezius). Similarly, both in dog and in humans homologous muscles have long fascicles and are adapted to large excursions. Furthermore, the internal architecture of the cervical vertebrae in quadrupeds was shown to be similar to that in humans (Smit, 2002). In particular, the vertebral trabeculae were found to course horizontally between the anterior and posterior endplates, implying that the main load on the vertebral body was axially compressive, similarly to the situation in humans, despite the radically different position of the spine in the two species (Smit, 2002). Because the gravitational loads in the dog (weight of the head and neck) are not compressive, this finding can only be due to loads from muscle and ligament forces. We thus conclude that the canine cervical region may be used as a modelling tool for biomechanical investigations of the human neck as long as the differences listed are borne in mind.

Acknowledgements

We thank Dr Francis J. Richmond (Department of Molecular Pharmacology and Toxicology, University of Southern California, Los Angeles) for making valuable suggestions to the preparation of this manuscript. We also thank Dr Walter Herzog (Human Performance Laboratory, Faculty of Kinesiology, University of Calgary, Calgary), and Dr Ori Brenner (The Weizmann Institute of Science, Rehovot, Israel) for technical assistance. We gratefully acknowledge Gal Shahak for creating excellent illustrations.

References

- Cheng EJ, Scott SH (2000) Morphometry of *Macaca mulatta* forlimb. I. Shoulder and elbow muscles and segment inertial parameters. *J Morph* **245**, 206–224.
- Cuts A (1988) Shrinkage of muscle fibres during fixation of cadaveric tissue. *J Anat* **160**, 75–78.
- Delp SI, Suryanarayanan S, Murray WM, Uhlir J, Triolo RJ (2001) Architecture of the rectus abdominis, quadratus lumborum and erector spinae. *J Biomech* **34**, 371–375.

- Deng YC, Goldsmith W** (1987) Response of a human head/neck/upper-torso replica to dynamic loading-II. Analytical/numerical model. *J Biomech* **20**, 487–497.
- Dumas GA, Poulin MJ, Roy B, Gagnon M, Jovanovic M** (1991) Orientation and moment arm of some trunk muscles. *Spine* **16**, 293–303.
- Engstrom CM, Loeb GE, Reid JG, Forrest WJ, Avruch L** (1991) Morphometry of the human thigh muscles. A comparison between anatomical sections and computer tomographic and magnetic resonance images. *J Anat* **176**, 139–156.
- Evans HE, Christensen GC** (1993) *Miller's Anatomy of the Dog*. Philadelphia: W.B. Saunders Co, pp. 279–329.
- Friederich JA, Brand RA** (1990) Muscle fiber architecture in the human lower limb. *J Biomech* **23**, 91–95.
- Gellman KS, Bertram JEA, Hermanson JW** (2002) Morphology, histochemistry, and function of epaxial cervical musculature in the horse (*Equus caballus*). *J Morph* **251**, 182–194.
- Gooding MR, Wilson CB, Hoff JT** (1975) Experimental cervical myelopathy. Effects of ischemia and compression of the canine cervical spinal cord. *J Neurosurg* **43**, 9–17.
- Graf W, De Waele C, Vidal PP** (1995) Functional anatomy of the head–neck movement system of quadrupedal and bipedal mammals. *J Anat* **185**, 55–74.
- Gray H** (1980) Myology. In *Gray's Anatomy* (eds Williams PL, Warwick, R), pp. 529–564. New York: Churchill Livingstone.
- Herzog W, Kamal S, Clark HD** (1992) Myofibril lengths of cat skeletal muscle: theoretical considerations and functional implications. *J Biomech* **25**, 945–948.
- Johnson GR, Spalding D, Nowitzke A, Bogduk N** (1996) Modeling the muscles of the scapula: morphometric and coordinate data and functional implications. *J Biomech* **29**, 1039–1051.
- Kamibayashi LK, Richmond FJR** (1998) Morphometry of human neck muscles. *Spine* **23**, 1314–1323.
- Keshner EA, Staler KD, Delp SL** (1997) Kinematics of the freely moving head and neck in the alert cat. *Exp Brain Res* **115**, 257–266.
- Klein Breteler MD, Spoor CW, Van der Helm FC** (1999) Measuring muscle and joint geometry parameters of a shoulder for modeling purposes. *J Biomech* **32**, 1191–1197.
- Kumaresan S, Yoganandan N, Pintar FA** (1999) Finite element analysis of the cervical spine: a material property sensitivity study. *Clin Biomech* **14**, 41–53.
- Li S, Vasavada AN, Delp SL, Peterson BW** (1995) A biomechanical model of the human head and neck musculoskeletal system. *Proceedings of the International Symposium on the Head–Neck System, Vail, Colorado, July 2–6, 1995*.
- Lieber RL, Friden J** (2000) Functional and clinical significance of skeletal muscle architecture. *Muscle Nerve* **23**, 1647–1666.
- Lieber RL, Friden J** (2001) Clinical significance of skeletal muscle architecture. *Clin Orthop Relat Res* **383**, 140–151.
- Mendez J, Keys A** (1960) Density and composition of mammalian muscle. *Metabolism* **9**, 184–188.
- Nickel R, Schummer A, Seiferle E, Frewein J, Wilkens H, Wille KH** (1986) Musculature of the torso. In *The Anatomy of the Domestic Animals, Vol. 1. the Locomotor System of the Domestic Mammals* (ed. Nickel R), pp. 265–298. Berlin: Verlag Paul Parey.
- Otten B** (1988) Concepts and models of functional architecture in skeletal muscle. *Exerc Sport Sci Rev* **16**, 89–137.
- Panjabi MM, Pelker R, Crisco JJ, Thibodeau L, Yamamoto I** (1988) Biomechanics of healing of posterior cervical spinal injuries in a canine model. *Spine* **13**, 803–807.
- Payne RC, Hutchinson JR, Robilliard JJ, Smith NC, Wilson AM** (2005a) Functional specialisation of pelvic limb anatomy in horses (*Equus caballus*). *J Anat* **206**, 557–574.
- Payne RC, Veenman P, Wilson AM** (2005b) The role of the extrinsic thoracic limb muscles in equine locomotion. *J Anat* **206**, 193–204.
- Raikova RT, Prilutsky BI** (2001) Sensitivity of predicted muscle forces to parameters of optimization-based human leg model revealed by analytical and numerical analyses. *J Biomech* **34**, 1243–1255.
- Richmond FJR, Vidal PP** (1990) The motor system. Joints and muscles of the neck. In *Control of Head Movement* (eds Peterson BW, Richmond FJR), pp. 1–21. New York: Oxford University Press.
- Richmond FJR** (1998) Element style in neuromuscular architecture. *Am Zool* **38**, 729–741.
- Richmond FJR, Liinamaa TA, Keane J, Thomson DB** (1999) Morphometry, histochemistry, and innervation of cervical shoulder muscles in the cat. *J Morph* **239**, 255–269.
- Richmond FJR, Singh K, Corneil BD** (2001) Neck muscles in the Rhesus monkey. I. Muscle morphometry and histochemistry. *J Neurophysiol* **86**, 1717–1728.
- Runciman RJ, Richmond FJR** (1997) Shoulder and forelimb orientations and loading in sitting cats: Implications for head and shoulder movement. *J Biomech* **30**, 911–919.
- Sacks RD, Roy RR** (1982) Architecture of the hind limb muscles of cats: functional significance. *J Morph* **173**, 185–195.
- Schmidt-Nielsen K** (1984) Problems of size and scale. In *Scaling: Why Is Animal Size So Important?* (ed. Schmidt-Nielsen K), pp. 7–32. Cambridge: Cambridge University Press.
- Selbie WS, Thomson DB, Richmond FJR** (1993) Suboccipital muscles in the cat neck: morphometry and histochemistry of the rectus capitis muscle complex. *J Morph* **216**, 47–63.
- Shahar R, Milgram J** (2005) Morphometric and anatomic study of the forelimb of the dog. *J Morph* **263**, 107–117.
- Sharp NJH, Cofone MT, Robertson ID, DeCarlo Smith G, Kornegay JN** (1989) Cervical spondylomyelopathy in the Doberman dog: a potential model for cervical spondylotic myelopathy in humans. *J Invest Surg* **2**, 333–339.
- Smit TH** (2002) The use of a quadruped as an in vivo model for the study of the spine – biomechanical considerations. *Eur Spine J* **11**, 137–144.
- Snijders CJ, Hoek van Dijke GA, Roosch ER** (1991) A biomechanical model for the analysis of the cervical spine in static postures. *J Biomech* **24**, 783–792.
- Stokes IAF, Gardner-Morse M** (1999) Quantitative anatomy of the lumbar musculature. *J Biomech* **32**, 311–316.
- Tobias PV** (1992) The upright in hominid evolution. In *The Head–Neck Sensory Motor System* (eds Berthoz A, Graf W, Vidal, PP), pp. 5–13. New York: Oxford University Press.
- Tsuang YH, Novak GJ, Schipplein OD, Hafezi A, Trafimow JH, Anderson GBJ** (1993) Trunk muscle geometry and centroid location when twisting. *J Biomech* **26**, 537–546.
- Van der Helm FC, Veenbaas R** (1991) Modeling the mechanical effect of muscles with large attachment sites: application to the shoulder mechanism. *J Biomech* **24**, 1151–1163.
- Vasavada AN, Li S, Delp SL** (1996) Variation in neck muscle

- fascicle lengths with head position. *Presented at the 20th Annual Meeting of the American Society of Biomechanics, Atlanta, Georgia, October 17–19, 1996.*
- Veeger HE, Van Der Helm FC, Van Der Woude LH, Pronk GM, Rozendal RH** (1991) Inertia and muscle contraction parameters for musculoskeletal modeling of shoulder mechanism. *J Biomech* **24**, 615–629.
- Villarraga ML, Anderson RC, Hart RT, Dinh DH** (1999) Contact analysis of a posterior cervical spine plate using a three-dimensional canine finite element model. *J Biomech Eng* **121**, 206–214.
- White AA, Johnson RM, Panjabi MM, Southwick WO** (1975) Biomechanical analysis of clinical stability in the cervical spine. *Clin Orth Rel Res* **109**, 85–96.
- Whitehill R, Barry JC** (1985) The evolution of stability in cervical spine constructs using either autogenous bone graft or methylmethacrylate cement: a follow-up report on a canine in-vivo model. *Spine* **10**, 32–41.
- Wickiewicz TL, Roy RR, Powell PL, Edgeron VR** (1983) Muscle architecture of the human lower limb. *Clin Orth Rel Res* **179**, 275–283.
- Winters JM** (1988) Biomechanical modeling of the human head and neck. In *Control of Head Movement* (eds Peterson BW, Richmond FJR), pp. 22–36. New York: Oxford University Press.
- Winters JM, Peles JD** (1990) Neck muscle activity and 3-D head kinematics during quasi-static and dynamic tracking movements. In *Multiple Muscle Systems: Biomechanics and Movement Organization* (eds Winters JM, Woo SL-Y), pp. 461–464. New York: Springer.
- Yoganandan N, Kumaresan S, Pintar FA** (2001) Biomechanics of the cervical spine: Part 2. Cervical spine soft tissue responses and biomechanical modeling. *Clin Biomech* **16**, 1–27.
- Zajac FE** (1989) Muscle and tendon: properties, models, scaling, and application to biomechanics and motor control. *Crit Rev Biomed Eng* **17**, 359–411.
- Zajac FE, Gordon ME** (1989) Determining muscle's force and action in multi-articular movement. *Exerc Sport Sci Rev* **17**, 187–230.